AGU PUBLICATIONS

Water Resources Research

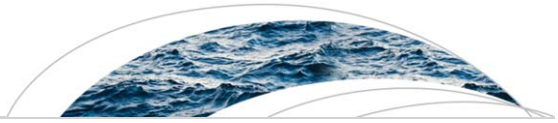

RESEARCH ARTICLE

10.1002/2018WR022546

Key Points:
- Preprocessing, data assimilation, and postprocessing experiments are conducted systematically with both synthetic and real data
- The precipitation error parameter has the most significant impact on the accuracy of streamflow predictions using the ensemble Kalman filter
- There is considerable temporal variation in the sensitivity of model parameters during the period of hydrologic predictions

Supporting Information:
- Supporting Informatation S1
- Data Set S1

Correspondence to:
S. Wang,
shuo.s.wang@polyu.edu.hk

Citation:
Wang, S., Ancell, B. C., Huang, G. H., & Baetz, B. W. (2018). Improving robustness of hydrologic ensemble predictions through probabilistic pre- and post-processing in sequential data assimilation. *Water Resources Research*, *54*, 2129–2151. https://doi.org/10.1002/2018WR022546

Received 9 JAN 2018
Accepted 2 MAR 2018
Accepted article online 8 MAR 2018
Published online 23 MAR 2018

Improving Robustness of Hydrologic Ensemble Predictions Through Probabilistic Pre- and Post-Processing in Sequential Data Assimilation

S. Wang[1], B. C. Ancell[2], G. H. Huang[3], and B. W. Baetz[4]

[1]Department of Land Surveying and Geo-Informatics, Hong Kong Polytechnic University, Hong Kong, China, [2]Department of Geosciences, Texas Tech University, Lubbock, TX, USA, [3]Faculty of Engineering and Applied Science, University of Regina, Regina, SK, Canada, [4]Department of Civil Engineering, McMaster University, Hamilton, ON, Canada

Abstract Data assimilation using the ensemble Kalman filter (EnKF) has been increasingly recognized as a promising tool for probabilistic hydrologic predictions. However, little effort has been made to conduct the pre- and post-processing of assimilation experiments, posing a significant challenge in achieving the best performance of hydrologic predictions. This paper presents a unified data assimilation framework for improving the robustness of hydrologic ensemble predictions. Statistical pre-processing of assimilation experiments is conducted through the factorial design and analysis to identify the best EnKF settings with maximized performance. After the data assimilation operation, statistical post-processing analysis is also performed through the factorial polynomial chaos expansion to efficiently address uncertainties in hydrologic predictions, as well as to explicitly reveal potential interactions among model parameters and their contributions to the predictive accuracy. In addition, the Gaussian anamorphosis is used to establish a seamless bridge between data assimilation and uncertainty quantification of hydrologic predictions. Both synthetic and real data assimilation experiments are carried out to demonstrate feasibility and applicability of the proposed methodology in the Guadalupe River basin, Texas. Results suggest that statistical pre- and post-processing of data assimilation experiments provide meaningful insights into the dynamic behavior of hydrologic systems and enhance robustness of hydrologic ensemble predictions.

Plain Language Summary Data assimilation techniques are recognized as a promising tool for probabilistic hydrologic predictions. And the pre- and post-processing of assimilation experiments play a crucial role in advancing our understanding of the nonlinear dynamic behavior of hydrologic prediction systems. This paper presents a unified computational framework that enables a systematic integration of data assimilation using the ensemble Kalman filter (EnKF) as well as statistical pre- and post-processing techniques, strengthening our capability in providing probabilistic streamflow predictions. Both synthetic and real data assimilation experiments are conducted to demonstrate applicability of the proposed computational framework in the Guadalupe River basin, Texas. Results verify that the pre- and post-processing of assimilation experiments provide meaningful insights into the potential interactions among the EnKF error parameters and those among hydrologic model parameters. In addition, the Gaussian anamorphosis establishes a seamless bridge between data assimilation and uncertainty quantification. Therefore, such a unified computational framework has significant potential for performing robust hydrologic forecasting.

1. Introduction

Hydrologic models are simplified representations of spatially and temporally varying hydrologic processes. As a result, uncertainty originates from various sources, including the errors in model structures and parameters, boundary and initial conditions, and hydrometeorological forcing (Ajami et al., 2007). It is thus necessary to characterize and communicate inevitable uncertainties in hydrologic predictions in order to provide reliable hydrologic data and information for sound planning and management of water resources.

Over the past decade, data assimilation techniques that combine observations with model forecasts to estimate the state of a physical system have been recognized as a useful means to quantify uncertainty and improve predictive accuracy (Gharamti et al., 2013; Khan & Valeo, 2016; Panzeri et al., 2014; Randrianasolo

et al., 2014; Ryu et al., 2009; Wang et al., 2017). The ensemble Kalman filter (EnKF) introduced by Evensen (1994) is a sequential data assimilation technique, which has been extensively used for state and parameter estimation of hydrologic models (Cammalleri & Ciraolo, 2012; DeChant & Moradkhani, 2012; Gharamti et al., 2015; Liu et al., 2016; Pathiraja et al., 2016b; Rafieeinasab et al., 2014; Xie & Zhang, 2010). For instance, Moradkhani et al. (2005) proposed the dual state-parameter estimation of hydrologic models using the EnKF. Wang et al. (2009) developed a constrained EnKF framework for state and parameter estimation in hydrologic modeling, in which the naive method, the projection and accept/reject methods were used to deal with inequality constraints. Samuel et al. (2014) evaluated the variations and forecasts of streamflow and soil moisture by using the EnKF with dual state-parameter estimation. Pathiraja et al. (2016a) investigated the potential for data assimilation by using the EnKF to detect known temporal patterns in model parameters from streamflow observations.

The EnKF has been increasingly applied in hydrologic modeling, which generates an ensemble of model states and parameters by adding stochastic perturbations (errors) to the forcing data and observations. Thus, properly tuning the EnKF error parameters plays a crucial role in hydrologic data assimilation, and has received considerable attention in the hydrologic modeling community over the past decade (De Lannoy et al., 2009; McMillan et al., 2013; Pauwels et al., 2013; Raleigh et al., 2015; Rasmussen et al., 2015, 2016; Zhang et al., 2016). For instance, Pauwels and De Lannoy (2009) performed the EnKF assimilation of discharge into conceptual rainfall-runoff models by adding Gaussian random errors to the meteorological forcings including precipitation and potential evapotranspiration, model parameters, and observations. De Lannoy and Reichle (2016) examined the random error parameters in the EnKF, and argued that the skill of land surface data assimilation systems can be improved through the optimal calibration of model and observation error parameters. Zhang et al. (2017) evaluated four different data assimilation methods for joint parameter and state estimation of the Variable Infiltration Capacity Model and the Community Land Model, and revealed that the errors in the forcing data and observations had a considerable contribution to the temporal fluctuations of the estimated parameter values. As a result, sensitivity experiments are often carried out for identifying error parameters and estimating the ensemble size (Clark et al., 2008; McMillan et al., 2013; Rasmussen et al., 2015; Sun et al., 2009; Yin et al., 2015). Nevertheless, univariate sensitivity analysis experiments are limited in determining the optimal settings of the EnKF. This is because the EnKF design parameters including error parameters and the ensemble size actually interact with each other in the data assimilation process, and their interactions have a considerable influence on the behavior of nonlinear dynamic systems. For instance, many of the highly sensitive parameters may provide redundant and misleading information regarding the variability of response variables because their sensitivities may be correlated with those of the other factors. As a result, failure to account for potential interactions among the EnKF design parameters can degrade the performance of the EnKF system (Crow & Loon, 2006; Thiboult & Anctil, 2015). It is thus necessary to perform a pre-processing of assimilation experiments for identifying the best EnKF settings so as to maximize the predictive performance. The variance-based global sensitivity analysis techniques such as the Sobol' method and the Fourier Amplitude Sensitivity Test are commonly used to estimate the key parameters and their interactions in hydrologic models (Dai & Ye, 2015; Pianosi & Wagener, 2016; Raleigh et al., 2015; Song et al., 2015). However, the variance-based sensitivity analysis can only indicate an overall interaction of each individual parameter through the total-order sensitivity index, and can hardly reveal the pairwise interactions between parameters. It is thus desired to further explore parameter interactions in order to advance our understanding of the model behavior in the parameter space.

Data assimilation using the EnKF can be performed to recursively derive the posterior distributions of model parameters; however, it can hardly explicitly characterize parameter interactions and their contributions to the predictive accuracy. To perform a robust parameter estimation and hydrologic prediction, it is necessary to perform a post-processing of assimilation experiments for revealing meaningful insights into the behavior of hydrologic prediction systems. Polynomial chaos expansion (PCE) is a well-known technique used to represent the evolution of uncertainty in stochastic dynamic systems, and has attracted great attention of hydrologists in recent years (Ciriello et al., 2013; Dai et al., 2016; Müller et al., 2011; Sochala & Le Maître, 2013). For instance, Fajraoui et al. (2011) investigated the effects of uncertain parameters on the output of a chosen interpretive solute transport model by using global sensitivity analysis together with the PCE methodology. Rajabi et al. (2015) performed a moment independent sensitivity analysis of seawater intrusion simulations by using the non-intrusive PCE. Wang et al. (2015a) proposed a two-stage factorial PCE

framework for quantifying interactive uncertainties in hydrologic predictions. Consequently, the PCE can be used as a promising post-processing tool for improving the robustness of hydrologic ensemble predictions through data assimilation.

In this work, we develop a unified data assimilation framework for enhancing the robustness of hydrologic ensemble predictions. Statistical pre-processing of assimilation experiments will be performed through the factorial design and analysis (FDA) to identify the best settings of the EnKF design parameters with maximized performance. When the posterior distributions of hydrologic model parameters are estimated, statistical post-processing experiments will also be conducted to explicitly reveal parameter interactions and to efficiently characterize predictive uncertainties. Both synthetic and real data assimilation experiments will be carried out to demonstrate feasibility and applicability of the proposed methodology in the Guadalupe River basin, Texas.

This paper is organized as follows. Section 2 describes the unified data assimilation framework for achieving robust hydrologic ensemble predictions. Section 3 provides details on the setup of synthetic and real data assimilation experiments as well as on the design of pre- and post-processing experiments. Section 4 presents a thorough analysis and discussion based on the results obtained from pre-processing, data assimilation, and post-processing experiments with both synthetic and real data. Finally, conclusions drawn from this study are summarized in section 5.

2. Development of a Unified Data Assimilation Framework

The unified data assimilation framework consists of three major parts (as shown in Figure 1), including statistical pre-processing, data assimilation with the EnKF, and statistical post-processing experiments. An overview of the steps involved in the unified computational framework is provided as follows: 1) selection of the EnKF design parameters, 2) design of the EnKF experiments, 3) execution of data assimilation experiments, 4) examination of sensitivities of the EnKF design parameters and their interactions, 5) identification of the best EnKF settings, 6) inference of posterior distributions of hydrologic model parameters, 7) transformation of posterior parameter distributions into normal distributions, 8) quantification of predictive uncertainties, and 9) investigation of dynamic sensitivities of parameter interactions affecting the predictive accuracy. Such a unified computational framework improves the robustness and effectiveness of hydrological ensemble predictions through probabilistic pre- and post-processing in the EnKF data assimilation.

2.1. Ensemble Kalman Filter

The basic idea of data assimilation is to merge information from models and observations so as to reduce and quantify uncertainty in model predictions. The EnKF is a sophisticated data assimilation technique that can be used for recursive estimation of hydrologic model parameters and state variables. In contrast to the extended Kalman filter (EKF), the EnKF makes use of Monte Carlo integration methods to approximate the error covariance matrix through a stochastic ensemble of model realizations instead of an explicit mathematical expression (Evensen, 2003). Thus, the EnKF is particularly useful for nonlinear dynamic models. By using the EnKF, the ensemble of model states is integrated forward in time to predict error statistics, and the model forecast can be made as follows:

$$x_{i,t+1}^{-} = f\left(x_{i,t}^{+}, u_{i,t+1}, \theta_{i,t+1}^{-}\right) + \omega_{i,t+1}, \tag{1}$$

where $x_{i,t+1}^{-}$ is predicted model state of ensemble number i at the current time step $t+1$, $x_{i,t}^{+}$ is the posterior model state of ensemble number i at the previous time step t, $u_{i,t+1}$ and $\theta_{i,t+1}$ are model inputs and parameters, respectively. f is the forward model that propagates state variables from time t to $t+1$, and $\omega_{i,t+1}$ is the model error that follows a Gaussian distribution with zero mean and covariance $\sum_{t+1}^{m}$. Since the model error is caused by uncertainties in model inputs, model structure and parameter values, it can be assumed to be a Gaussian random perturbation with zero mean and standard deviation of 0.1. As for the recursive parameter estimation by using the EnKF, it is assumed that model parameters are perturbed by a small random noise:

$$\theta_{i,t+1}^{-} = \theta_{i,t}^{+} + \tau S(\theta_{i,t}^{-}), \tag{2}$$

where τ is a small tuning parameter (0.01 is used in this study), and $S(\theta_{i,t}^{-})$ is the standard deviation of the prior parameter distribution in such a way that the parameter estimation at the current time step always

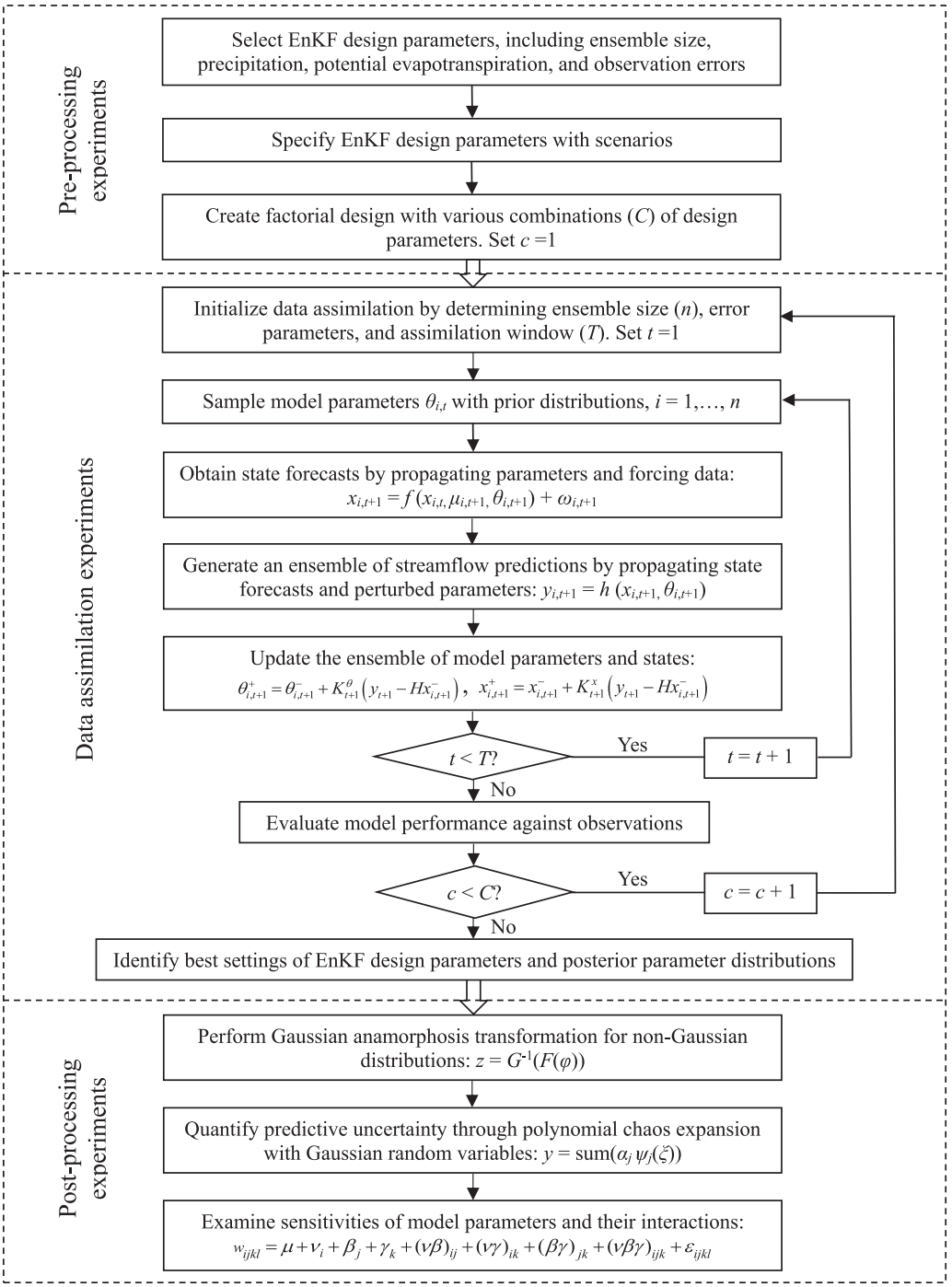

Figure 1. Flowchart for the unified data assimilation framework. *T* and *C* represent the assimilation window and the factorial combination, respectively.

takes into account the prior parameter information estimated at the previous time step as the model progresses forward in time (DeChant & Moradkhani, 2012).

The ensemble members of model states and parameters can then be updated as follows:

$$x^{+}_{i,t+1} = x^{-}_{i,t+1} + K^{x}_{t+1}\left(y_{t+1} - Hx^{-}_{i,t+1}\right), \tag{3}$$

$$\theta_{i,t+1}^{+}=\theta_{i,t+1}^{-}+K_{t+1}^{\theta}\left(y_{t+1}-Hx_{i,t+1}^{-}\right), \tag{4}$$

where y_{t+1} is the observation vector, H is the observation operator that converts model states to the observation space, and K_{t+1}^{x} and K_{t+1}^{θ} are the Kalman gain matrices for model states and parameters, respectively. K_{t+1}^{x} and K_{t+1}^{θ} can be written by:

$$K_{t+1}^{x}=P_{t+1}^{x}H_{t+1}^{\mathrm{T}}\left(H_{t+1}P_{t+1}^{x}H_{t+1}^{\mathrm{T}}+R_{t+1}\right)^{-1}, \tag{5}$$

$$K_{t+1}^{\theta}=P_{t+1}^{\theta}H_{t+1}^{\mathrm{T}}\left(H_{t+1}P_{t+1}^{\theta}H_{t+1}^{\mathrm{T}}+R_{t+1}\right)^{-1}, \tag{6}$$

where P_{t+1}^{x} and P_{t+1}^{θ} are the state error covariance and the parameter error covariance, respectively. R_{t+1} is the observation error covariance, and superscript T denotes the matrix transpose. P_{t+1}^{x} and P_{t+1}^{θ} can be computed by:

$$P_{t+1}^{x}=E\left[\left(x_{i,t+1}^{-}-\bar{x}_{t+1}^{-}\right)\left(x_{i,t+1}^{-}-\bar{x}_{t+1}^{-}\right)^{\mathrm{T}}\right], \tag{7}$$

$$P_{t+1}^{\theta}=E\left[\left(\theta_{i,t+1}^{-}-\bar{\theta}_{t+1}^{-}\right)\left(\theta_{i,t+1}^{-}-\bar{\theta}_{t+1}^{-}\right)^{\mathrm{T}}\right]. \tag{8}$$

where $\bar{x}_{t+1}^{-}$ and $\bar{\theta}_{t+1}^{-}$ represent the state ensemble mean and the parameter ensemble mean, respectively. E is the expectation operator.

As for hydrologic data assimilation using the EnKF, the ensemble of model trajectories is produced by stochastically perturbing the forcing data, leading to the uncertainty in model outputs. Thus, specifying the error parameters (magnitude of perturbations) and the ensemble size plays a crucial role in the performance of the EnKF.

2.2. Factorial Design and Analysis

Factorial design and analysis (FDA) is a powerful statistical method for examining the effects of multiple factors on response variables through experimental design and data analysis (Montgomery & Runger, 2013). In a factorial experiment, all possible combinations of the levels of factors are examined in order to reveal potential interactions among multiple factors.

In this study, the FDA can be applied to data assimilation experiments for examining the effects of the EnKF design parameters on the predictive performance. As a result, the levels of experimental factors correspond to the scenarios of the EnKF design parameters including the ensemble size, the precipitation error, the potential evapotranspiration error and the observation error. The response variable represents the predictive accuracy in terms of root mean square error (RMSE). For instance, if there are a scenarios of the precipitation error, b scenarios of the potential evapotranspiration error, and c scenarios of the observation error, there will be a total of abc estimations of the RMSE values derived through hydrologic data assimilation in a complete factorial experiment. The effects model for such a factorial experiment with three parameters can be described by:

$$w_{ijkl}=\mu+v_i+\beta_j+\gamma_k+(v\beta)_{ij}+(v\gamma)_{ik}+(\beta\gamma)_{jk}+(v\beta\gamma)_{ijk}+\varepsilon_{ijkl}\quad\begin{cases}i=1,2,\ldots a\\ j=1,2,\ldots b\\ k=1,2,\ldots c\\ l=1,2,\ldots n\end{cases}, \tag{9}$$

where w_{ijkl} is the total variability in the RMSE values, μ is the overall mean effect for all error parameters, v_i is the effect of the precipitation error under the ith scenario, β_j is the effect of the potential evapotranspiration error under the jth scenario, γ_k is the effect of the observation error under the kth scenario, $(v\beta)_{ij}$ is the effect of the interaction between the precipitation error and the potential evapotranspiration error, $(v\gamma)_{ik}$ is the effect of the interaction between the precipitation error and the observation error, $(\beta\gamma)_{jk}$ is the effect of the interaction between the potential evapotranspiration error and the observation error, $(v\beta\gamma)_{ijk}$ is the effect of the interaction among the precipitation error, the potential evapotranspiration error, and the observation error, and ε_{ijkl} is the random error component which is normally distributed with mean 0 and variance σ^2.

The effects model contains three main parameter effects, three two-parameter interaction effects, a three-parameter interaction effect, and an error term. These effects can be defined as deviations from the overall mean, so $\sum_{i=1}^{a} v_i = 0$, $\sum_{j=1}^{b} \beta_i = 0$, $\sum_{k=1}^{c} \gamma_k = 0$, $\sum_{i=1}^{a} (v\beta)_{ij} = \sum_{j=1}^{b} (v\beta)_{ij} = 0$, $\sum_{i=1}^{a} (v\gamma)_{ik} = \sum_{k=1}^{c} (v\gamma)_{ik} = 0$, $\sum_{j=1}^{b} (\beta\gamma)_{jk} = \sum_{k=1}^{c} (\beta\gamma)_{jk} = 0$, and $\sum_{i=1}^{a} (v\beta\gamma)_{ijk} = \sum_{j=1}^{b} (v\beta\gamma)_{ijk} = \sum_{k=1}^{c} (v\beta\gamma)_{ijk} = 0$ (Montgomery, 2000).

In factorial experiments, the main effect is estimated as the difference between the average values of RMSE derived from different parameter scenarios. For instance, suppose that the precipitation error is given two scenarios, the main effect of the precipitation error can be computed by:

$$PE = \bar{m}_{P_1} - \bar{m}_{P_2}, \tag{10}$$

where PE represents the main effect of the precipitation error, and $\bar{m}_{P_1}$ and $\bar{m}_{P_2}$ represent the average values of RMSE derived under scenarios 1 and 2, respectively. Since an interaction occurs when the effect of one error parameter on the value of RMSE changes depending on the scenario of another error parameter, the effect of the pairwise interaction between the precipitation error and the observation error can be computed by:

$$PE \times OE = \frac{1}{2}\{[\bar{m}(P_2|O_2) + \bar{m}(P_1|O_1)] - [\bar{m}(P_2|O_1) + \bar{m}(P_1|O_2)]\}. \tag{11}$$

where $PE \times OE$ represents the pairwise interaction between the precipitation error and the observation error, $\bar{m}(P_1|O_1)$ represents the conditional value of RMSE derived under scenario 1 of the precipitation error when the observation error is given under scenario 1, $\bar{m}(P_2|O_2)$ represents the conditional value of RMSE derived under scenario 2 of the precipitation error when the observation error is given under scenario 2, $\bar{m}(P_2|O_1)$ represents the conditional value of RMSE derived under scenario 2 of the precipitation error when the observation error is given under scenario 1, and $\bar{m}(P_1|O_2)$ represents the conditional value of RMSE derived under scenario 1 of the precipitation error when the observation error is given under scenario 2. All the other main and interaction effects for error and model parameters can be estimated accordingly. The half-normal probability plot can then be used as a powerful graphic tool to identify the important parameter effects. In this plot, the half-normal distribution is created in the same way as the standard normal distribution with mean zero, except that only the positive half of the normal curve is considered. Thus, a positive normal value drawn from the half-normal distribution is given as the expected half-normal value for each value of parameter effects, ranked by increasing values. In other words, each parameter effect has an expected half-normal value in the half-normal probability plot where the important parameters are those whose effects are far away from zero while the unimportant parameters are those that have near-zero effects.

The FDA can be used as a promising pre-processing tool to identify the best EnKF settings with maximized performance. The EnKF can then be used to derive the posterior distributions of hydrologic model parameters. To further characterize predictive uncertainties, it is necessary to explore the forward propagation and evolution of parameter uncertainties in order to advance our understanding of the behavior of hydrologic systems.

2.3. Factorial Polynomial Chaos Expansion With Gaussian Anamorphosis

The polynomial chaos expansion (PCE), first introduced by Wiener (1938), can be used as a powerful tool to characterize the evolution of uncertainty in hydrologic modeling systems through a series expansion of orthogonal polynomials. By using the PCE, the probabilistic model output can be represented by:

$$y = a_0 + \sum_{i_1=1}^{\infty} a_{i_1} \Gamma_1(\xi_{i_1}) + \sum_{i_1=1}^{\infty} \sum_{i_2=1}^{i_1} a_{i_1 i_2} \Gamma_2(\xi_{i_1}, \xi_{i_2}) + \sum_{i_1}^{\infty} \sum_{i_2=1}^{i_1} \sum_{i_3=1}^{i_2} a_{i_1 i_2 i_3} \Gamma_3(\xi_{i_1}, \xi_{i_2}, \xi_{i_3}) + \cdots, \tag{12}$$

where y is the predicted streamflow, ξ_i is the model parameter expressed in the form of the standard normal random variable, α_0 and $a_{i_1 i_2, \ldots, i_d}$ are the PCE coefficients, and $\Gamma_d(\xi_{i_1}, \ldots, \xi_{id})$ are the multivariate Hermite polynomials of order d, which are the functions of random model parameters (Xiu & Karniadakis, 2002). The general expression of Hermite polynomials is given by:

$$\Gamma_d(\xi_{i_1}, \ldots, \xi_{i_d}) = (-1)^d e^{\frac{1}{2}\xi^T \xi} \frac{\partial^d}{\partial \xi_{i_1} \ldots \partial \xi_{i_d}} e^{-\frac{1}{2}\xi^T \xi}. \tag{13}$$

The PCE coefficients are obtained by using the probabilistic collocation method that equates the PCE and the corresponding model outputs at a set of selected collocation points (Li & Zhang, 2007). And the collocation points are selected from the roots of the Hermite polynomial of one degree higher than the order of

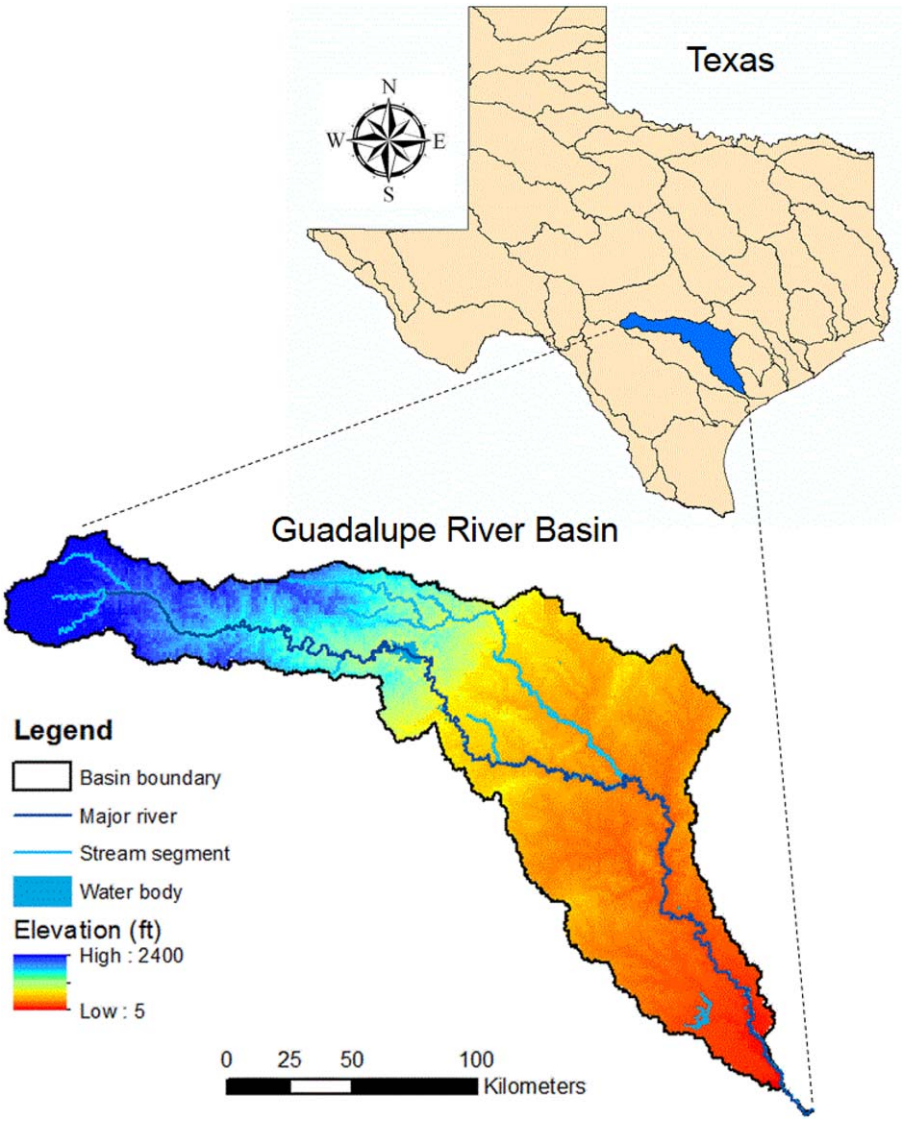

Figure 2. Geographical location and topographic characteristics of the Guadalupe River basin.

the given PCE (Tatang et al., 1997). To improve the robustness of PCE, Wang et al. (2015b) proposed a factorial polynomial chaos expansion (FPCE) which merged the strengths of the multi-factorial design and analysis as well as the probabilistic collocation method for characterizing the forward propagation of parameter uncertainties through hydrologic models. Thus, the FPCE can serve as an efficient approximation of a stochastic system to represent the uncertainties in model outputs by orthogonal polynomials. Moreover, the FPCE can explicitly reveal the pairwise interactions between model parameters affecting the predictive

Table 1
Initial Uncertainty Ranges of Model Parameters and Their "True" Values

Parameter	Description	Initial range	True value
C_{max} (mm)	Maximum storage capacity of watershed	[10, 1000]	635
b_{exp} (−)	Degree of spatial variability of soil moisture capacity	[0.0, 10.0]	1.65
β (−)	Factor distributing flow to the quick-flow tank	[0.0, 1.0]	0.3
R_s (days^{-1})	Residence time of the slow-flow tank	[0.0, 0.2]	0.1
R_q (days^{-1})	Residence time of the quick-flow tank	[0.1, 1.0]	0.4

performance, as well as the temporal variation in the parameter sensitivity during the period of hydrologic predictions. Thus, the FPCE can provide meaningful insights into the complex dynamics and chaos in hydrologic prediction systems.

Since the convergence rate of the Hermite polynomials is optimal for Gaussian processes, data transformation techniques are needed when the posterior parameter distributions derived through data assimilation

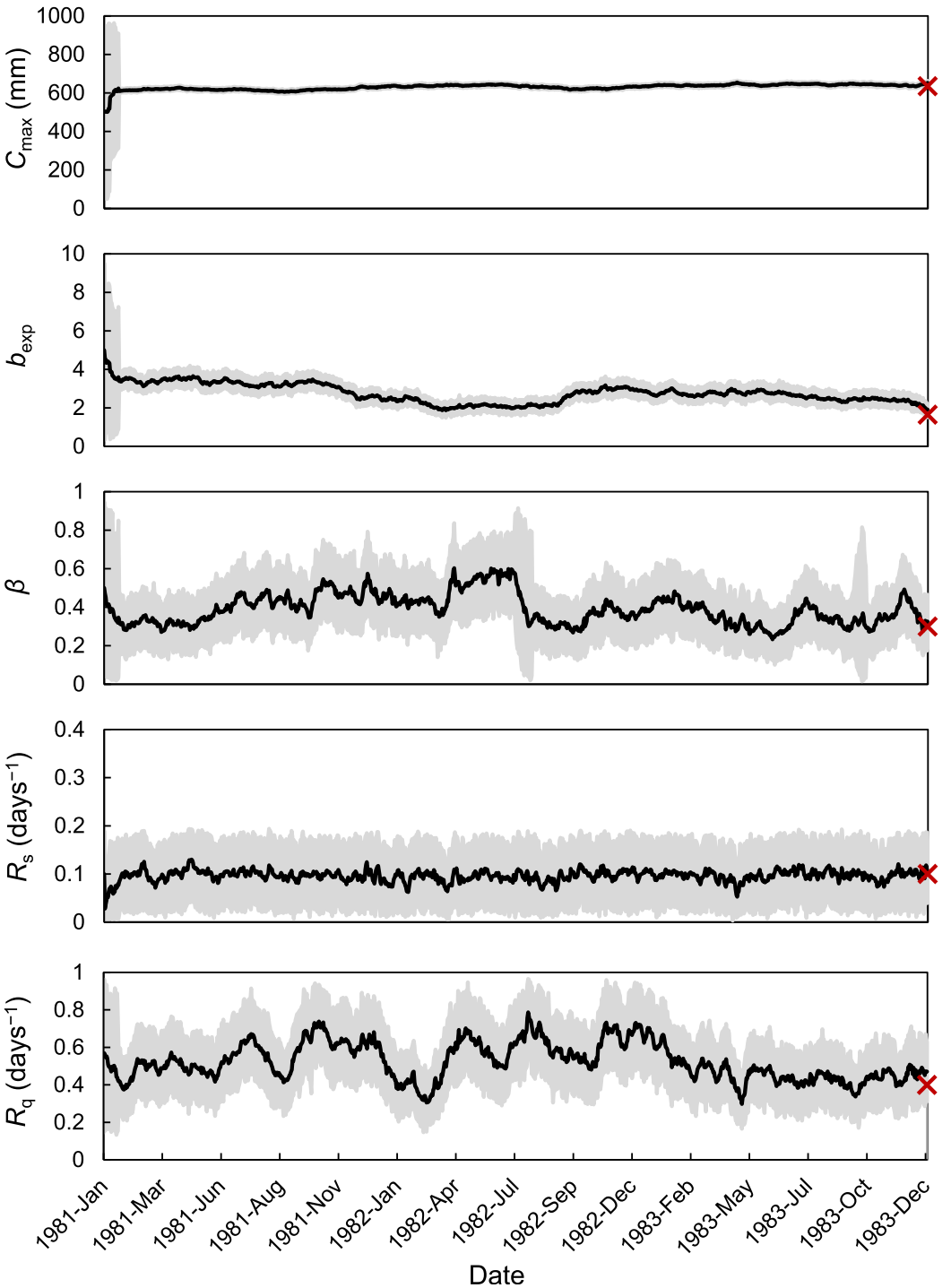

Figure 3. Convergence of model parameters to "true" values. Shaded areas and solid lines represent 90% confidence intervals and mean values, respectively. Crosses denote "true" parameter values.

are not well characterized by normal Gaussian probability density functions. The Gaussian anamorphosis is a powerful data transformation technique that can be used to establish a link between an arbitrarily distributed variable φ and its Gaussian transform variable z:

$$z = G^{-1}(F(\varphi)), \tag{14}$$

where G is the theoretical standard normal cumulative distribution function (CDF) of z, $F(\varphi)$ is the empirical CDF of φ, and can be obtained by (Johnson & Wichern, 1988; Schöniger et al., 2012):

$$F_j = \frac{j-0.5}{N}, \tag{15}$$

where N is the sample size, and j is the rank of the sample data. According to the empirical CDF F_j, the range of the sample data can be determined by:

$$z_{\min} = G^{-1}((1-0.5)/N), \tag{16}$$

$$z_{\max} = G^{-1}((N-0.5)/N). \tag{17}$$

When the data values lie outside the range from $z_{\min}$ to $z_{\max}$, the anamorphosis function can be extrapolated with a straight line that connects the lowest and the highest original data values and their respective transformed values (Schöniger et al., 2012). The Gaussian anamorphosis is useful for transforming the posterior parameter distributions into Gaussian distributions. The FPCE can then be applied as a statistical post-processing tool to explore parameter interactions and to characterize predictive uncertainties. Such a systematic computational framework enhances the robustness of hydrologic prediction systems.

3. Experimental Setup

The unified data assimilation framework was applied to predict daily streamflow in the Guadalupe River basin, south-central Texas. The Guadalupe River originates in Kerr County, and flows into the Guadalupe

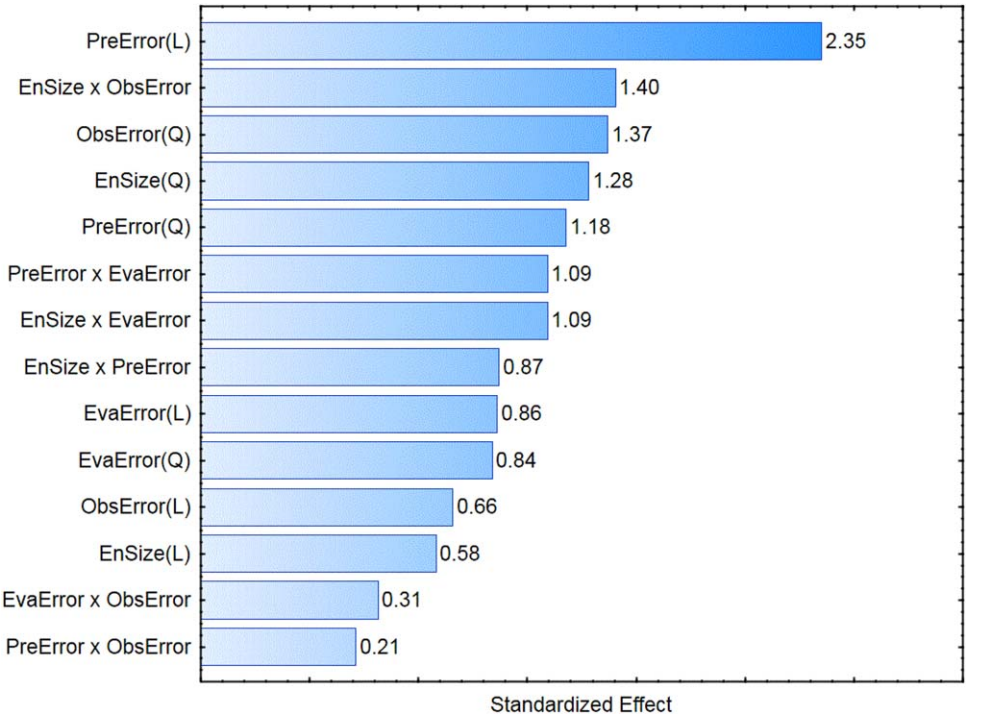

Figure 4. Estimate of standardized effects including main and interaction effects for the EnKF design parameters. EnSize, PreError, EvaError, and ObsError represent ensemble size, precipitation error, potential evapotranspiration error, and streamflow observation error, respectively. (L) and (Q) denote linear and quadratic effects, respectively.

Estuary with a mean daily discharge of 53 m^3/s. The river has a drainage area of about 15,500 km^2. Annual precipitation ranges from 770 mm near the headwaters to 1,000 mm near the Gulf of Mexico (Sharif et al., 2010). As shown in Figure 2, the Guadalupe River and its tributaries are a vital source of water for a number of populous cities, including Kerrville, New Braunfels, San Marcos, Seguin, Lockhart, Gonzales, Cuero, Luling, and Victoria. Streamflow conditions in the Guadalupe River basin are mainly affected by spring discharge, rainfall-runoff processes, evapotranspiration, withdrawals for water supply, reservoir operations, and losses to aquifer recharge (Ockerman & Slattery, 2008). The study area has a subtropical subhumid climate characterized by hot summers and dry winters. Heaviest rainfall often occurs in spring and early summer, but can occur anytime during the year. Thus, high and low rainfall periods are common, resulting in recurring floods and droughts.

3.1. Data and Model

In this study, the meteorological and hydrological data for the Guadalupe River basin were collected from the Model Parameter Estimation Experiment (MOPEX) data set (Duan et al., 2006). A total of four years of data from January 1980 to December 1983 were used to assimilate daily streamflow such that the first year was used as a spin-up period to reduce sensitivity to state-value initialization. Both synthetic and real data assimilation experiments were conducted to demonstrate feasibility and applicability of the proposed methodology. A synthetic experiment with predefined model parameters was first performed to generate the "true" model states, and then the EnKF data assimilation was conducted using the synthetic data set

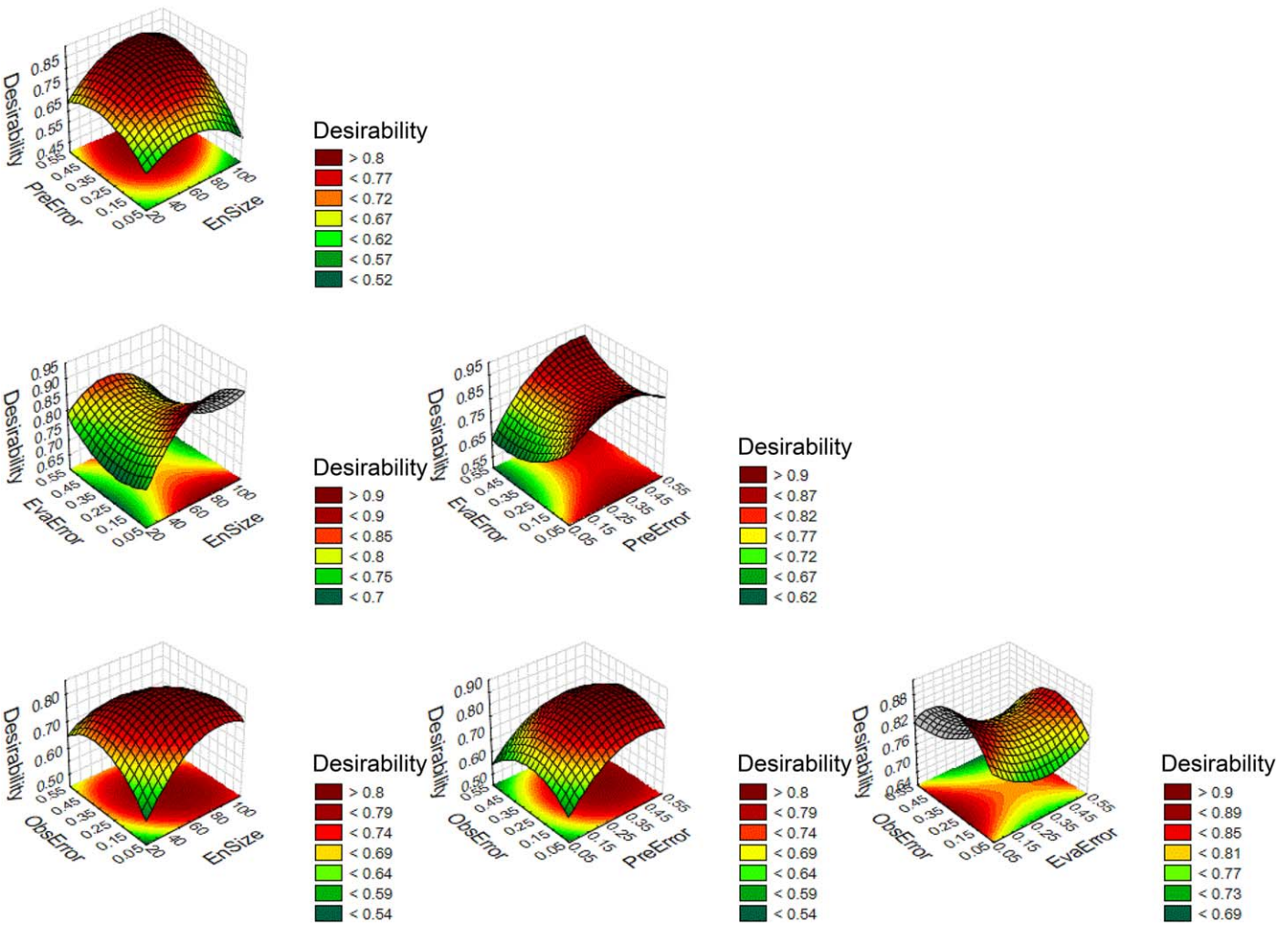

Figure 5. Desirability of model response for pairwise interactions between the EnKF design parameters. Desirability values range from 0.0 for an undesirable response to 1.0 for a highly desirable response.

such that the convergence of model parameters could be evaluated based on the predefined parameter values. The assimilation experiment with real streamflow data was then performed when the performance of the EnKF was validated.

Data assimilation experiments were conducted by using the HYMOD which is a widely used rainfall-runoff model for probabilistic hydrologic predictions (Bulygina & Gupta, 2011; Sadegh & Vrugt, 2013; Young, 2013). In the HYMOD, the runoff generation process partitions excess rainfall into surface storage characterized by three quick-flow tanks and subsurface storage represented by a single slow-flow tank through a partitioning factor (Moore, 2007). Thus, the total discharge from both quick- and slow-flow tanks is the generated streamflow in the river basin.

The HYMOD has five parameters, including the maximum soil moisture storage capacity C_{max}, the degree of spatial variability in the storage capacity b_{exp}, the factor to distribute flow between the quick- and slow-flow routing β, the residence time of the slow-flow tank R_s, and the residence time of quick-flow tanks R_q. The initial ranges of model parameters and their "true" values are given in Table 1. In addition, daily precipitation and potential evapotranspiration are the forcing input data used to drive the HYMOD model. To account for various sources of uncertainty through data assimilation using the EnKF, stochastic perturbations (representing errors) were applied to precipitation and potential evapotranspiration data as well as streamflow observations, leading to an ensemble of state variables. In this study, the precipitation error was assumed to have a log-normal distribution while the potential evapotranspiration and the streamflow observation errors were assumed to have normal distributions. As a result, the specification of error parameters and the ensemble size is a key feature of the EnKF, which plays an important role in the performance of hydrologic ensemble predictions.

3.2. Design of Statistical Pre- and Post-Processing Experiments

In this study, statistical pre-processing of data assimilation experiments was performed to identify the best settings of the EnKF design parameters including the ensemble size, the precipitation error, the potential

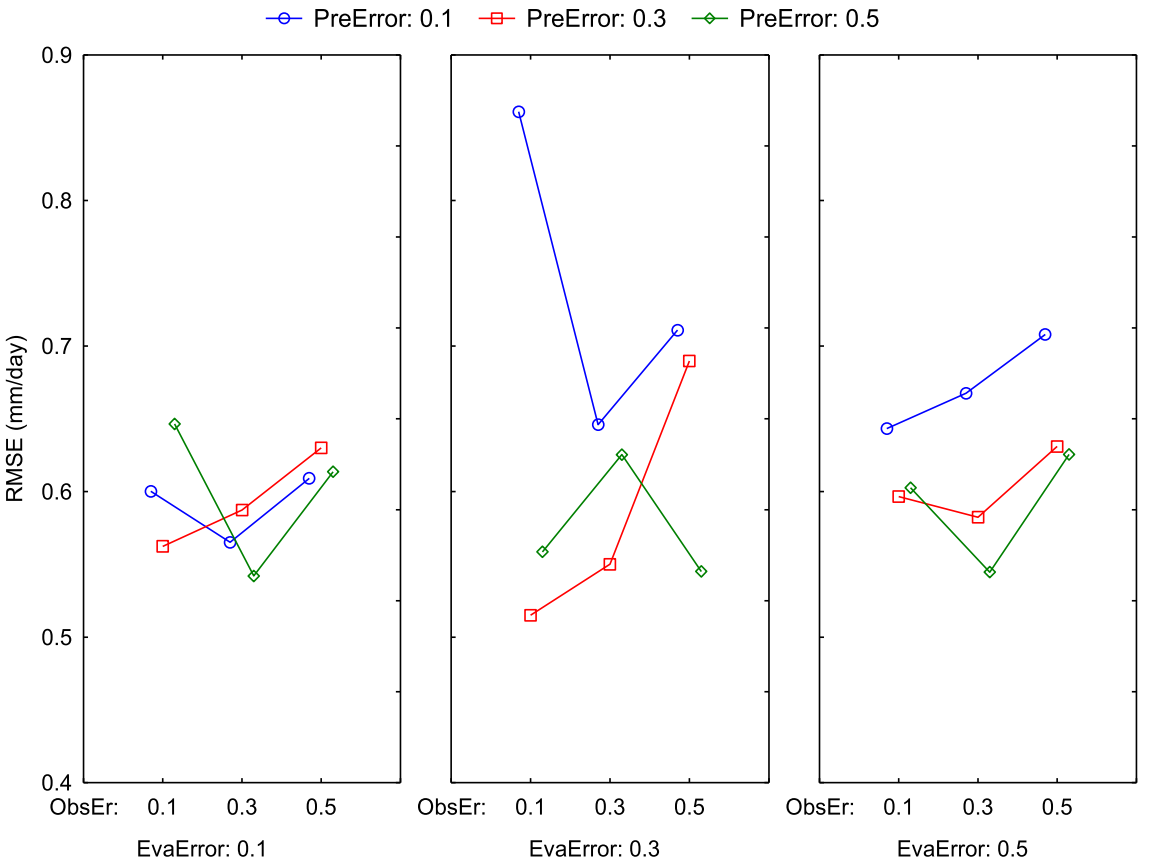

Figure 6. Three-way interactions among the EnKF error parameters.

evapotranspiration error, and the streamflow observation error. Three scenarios were given on the strength of perturbations (error standard deviations), including 0.1 mm/day, 0.3 mm/day, and 0.5 mm/day. In addition, the ensemble sizes of 30, 60, and 100 were used in combination with various error parameters in the pre-processing experiment. The FDA was performed to explicitly examine sensitivities of the EnKF design parameters affecting the predictive accuracy, which provides meaningful information for achieving the best performance of hydrologic data assimilation using the EnKF.

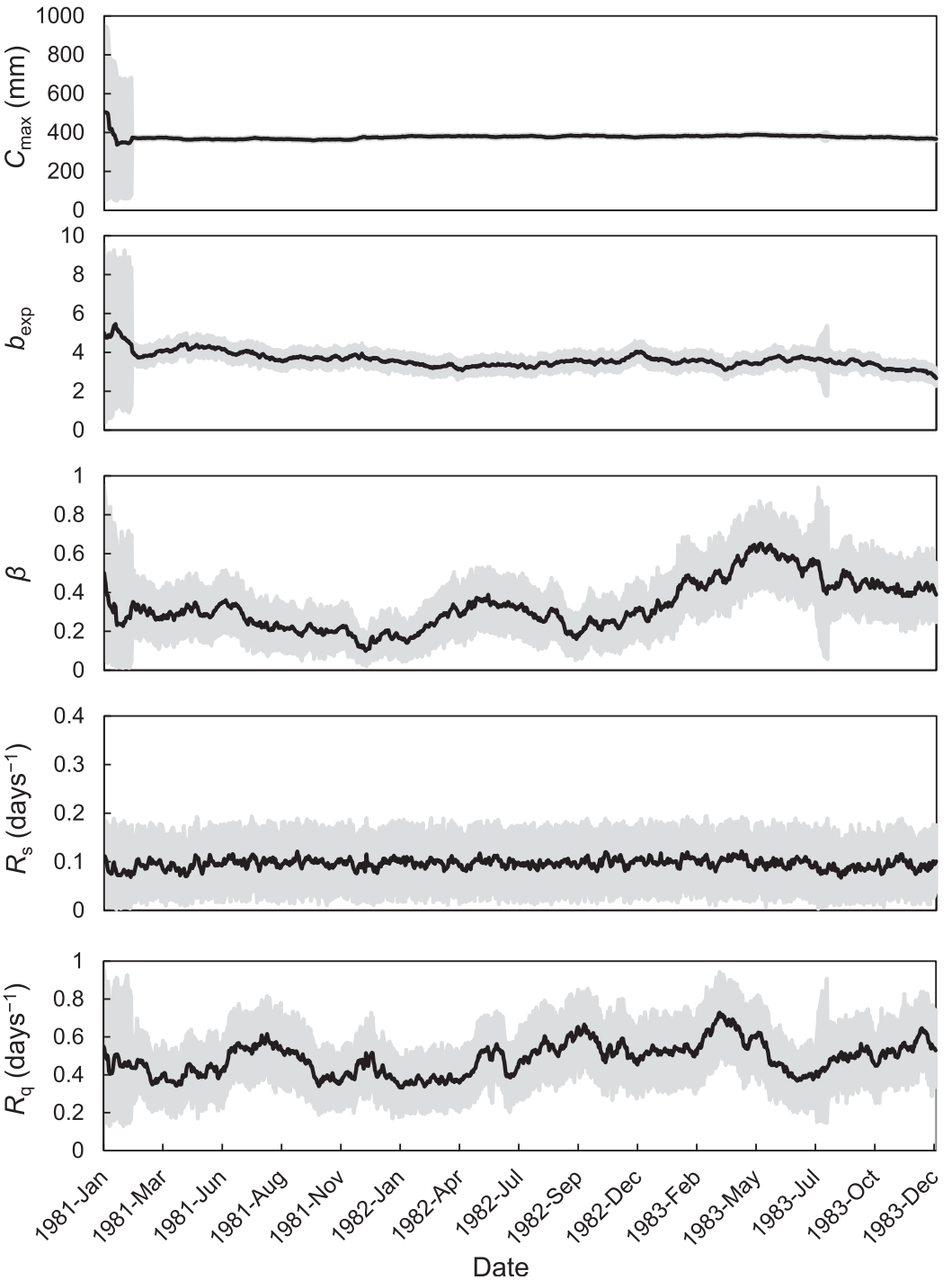

Figure 7. Temporal evolution of model parameters with 90% confidence intervals under the real data assimilation scenario.

When the posterior distributions of hydrologic model parameters were estimated, a statistical post-processing experiment was also performed to further reveal the dynamics of parameter interactions and sensitivities. Since the derived posterior parameter distributions can hardly be characterized by certain distributions such as normal and gamma distributions, the Gaussian anamorphosis can be used to transform posterior parameter distributions into normal distributions. The normally distributed parameters can then be propagated through the FPCE to efficiently produce probabilistic hydrologic predictions.

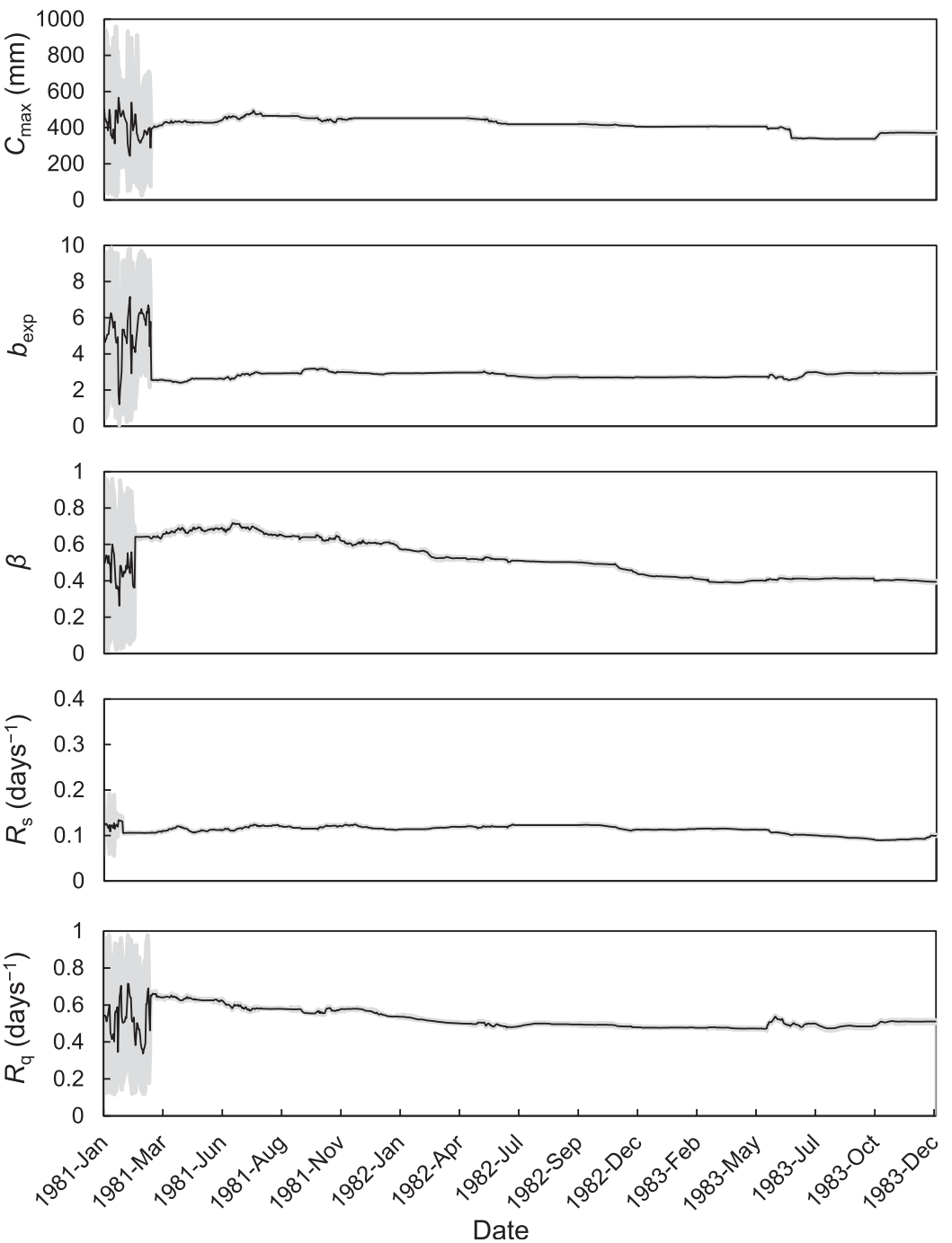

Figure 8. Temporal evolution of model parameters with 90% confidence intervals by using a weighted parameter sampling approach.

We took into account various sources of uncertainty in hydrologic predictions, including the EnKF design parameters, the forcing data and model parameters. However, the model structural error was not addressed in this study, which might lead to biased hydrologic predictions (Renard et al., 2010; Xu et al., 2017). Since both the EnKF design parameters and model parameters may be adjusted to compensate for the model structural error inherent in hydrologic predictions, it is desired to explicitly characterize the model structural error in future studies through a joint inference of model parameters and the structural error, enhancing the robustness of hydrologic predictions.

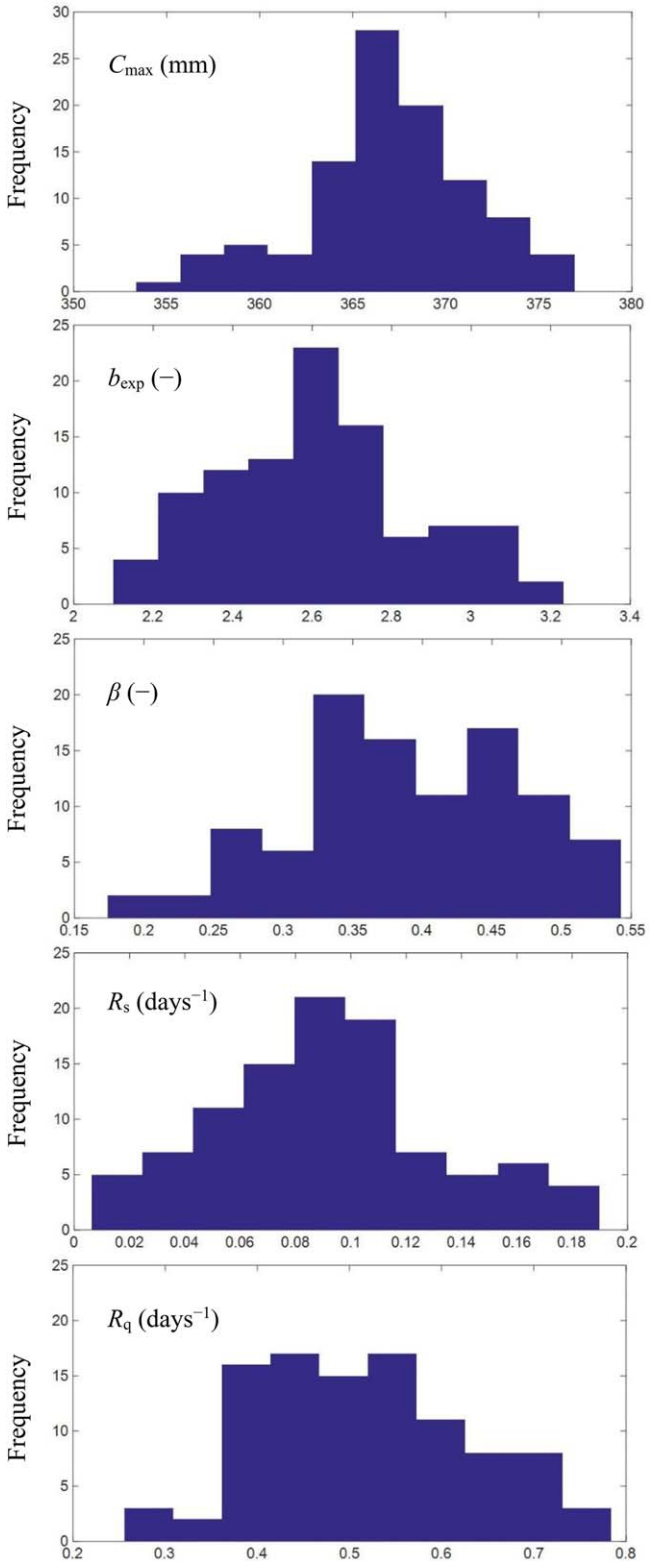

Figure 9. Posterior distributions of model parameters.

4. Results and Discussion

4.1. Assimilation of Synthetic Streamflow Data

A synthetic experiment was performed to examine the ability of the EnKF algorithm to estimate the predefined model parameters. Figure 3 depicts the convergence of model parameters over a three-year period. In terms of parameter identifiability, the first two parameters relating to the soil moisture storage capacity, denoted by C_{max} and b_{exp}, are easily identifiable, and they rapidly converge to the posterior target distributions at the early stage of the streamflow assimilation process. However, the uncertainty in the parameter estimation can be underestimated when the parameter ensemble spreads shrink too rapidly with a limited sample size, it is thus necessary to reduce the potential risk of sample depletion with a sufficient ensemble size. In comparison, the other three parameters including β, R_s and R_q are less identifiable with larger uncertainty bounds. It is thus desired to further analyze and characterize the uncertainty in streamflow predictions.

As the streamflow assimilation proceeds, the mean values of posterior parameter distributions converge toward the "true" values predefined as: $C_{max} = 635$ mm, $b_{exp} = 1.65$, $\beta = 0.3$, $R_s = 0.1$ days^{-1}, and $R_q = 0.4$ days^{-1}. Furthermore, the "true" values of all parameters are covered by the posterior confidence intervals derived through data assimilation. Results verify that the EnKF algorithm is able to properly estimate the "true" posterior parameters, and can thus be used for uncertainty assessment of hydrologic model parameters and predictions in the real data assimilation experiment.

4.2. Assimilation of Real Streamflow Data

When the performance of the EnKF algorithm was validated through the synthetic experiment, a real data assimilation experiment was conducted to predict daily streamflow in the Guadalupe River basin over the same period of three years. To optimize the predictive performance, the FDA was performed to identify the best settings of the EnKF by examining potential interactions among the EnKF design parameters. As shown in Figure 4, the precipitation error parameter has the most significant impact on the predictive accuracy. This indicates that any change in the precipitation error parameter could lead to the largest variation of the RMSE value. In addition, the streamflow observation error parameter, the ensemble size, and their interaction have relatively large contributions to the predictive performance.

Figure 5 explicitly depicts all pairwise interactions between the EnKF design parameters that affect the predictive performance using the RMSE value. The response surface of desirability is produced by fitting the predicted values of RMSE using a function based on different

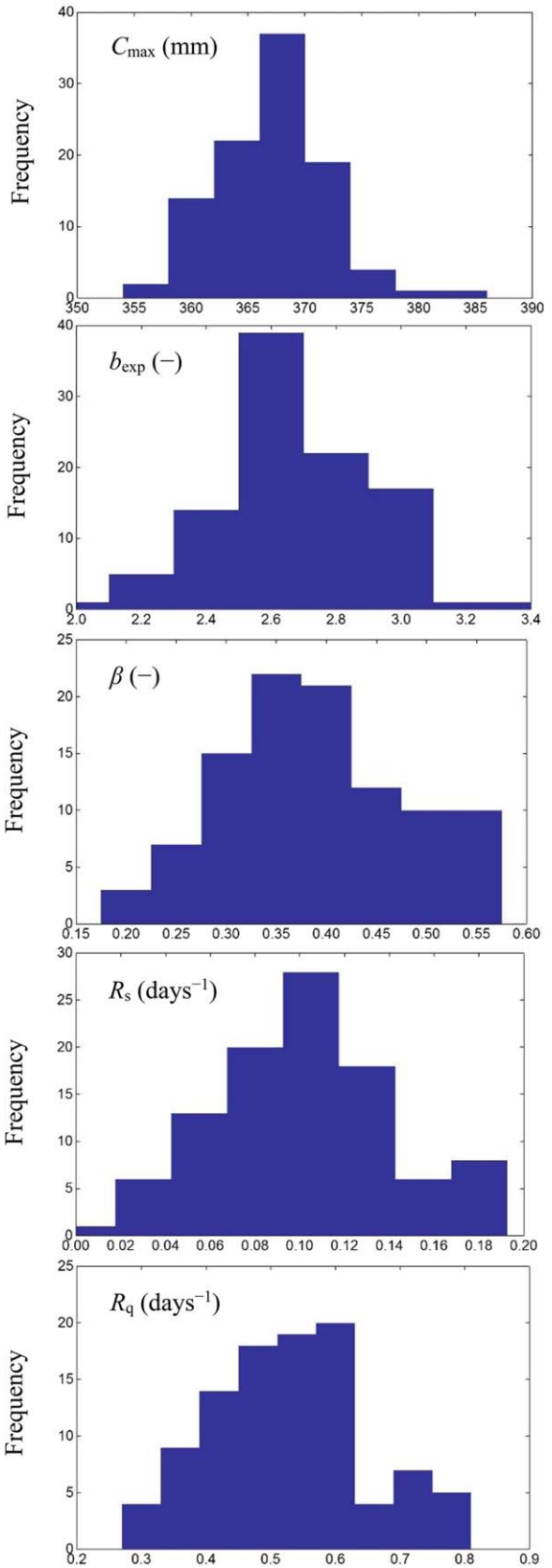

Figure 10. Estimation of the non-Gaussian characteristics of posterior distributions.

scenarios of the EnKF design parameters. In this study, the continuous response surface is created by using the spline function that is defined as a piecewise polynomial for interpolating discrete data points. The desirability scores range from 0.0 representing an undesirable response (i.e., largest RMSE value) to 1.0 representing a highly desirable response (i.e., smallest RMSE value). The pairwise interactions between the potential evapotranspiration error parameter and the other design parameters produce highly desirable response, especially for the interaction between the potential evapotranspiration error and the precipitation error parameters. In addition, when the ensemble size increases gradually, its interactions with other parameters tend to increase the desirability values accordingly.

Figure 6 shows the three-way interactions among the EnKF error parameters, and reveals their contributions to the predictive accuracy. The magnitude and direction of the interaction between the precipitation error and the streamflow observation error parameters vary dynamically depending on the settings of the potential evapotranspiration error parameter. Such a three-way interaction analysis reveals that the minimum value of RMSE would be obtained when the settings of the precipitation error, the evapotranspiration error, and the observation error parameters are 0.3 mm/day, 0.3 mm/day, and 0.1 mm/day, respectively. It is thus necessary to identify the best parameter settings through exploring dynamic interactions among the EnKF design parameters, which provides meaningful information for advancing our understanding of the EnKF data assimilation system and for maximizing the predictive performance. By using the FDA, the best EnKF settings can be identified as: the precipitation error = 0.3 mm/day, the evapotranspiration error = 0.3 mm/day, the observation error = 0.1 mm/day, and the ensemble size = 100.

Figure 7 shows the temporal evolution of hydrologic model parameters derived through the real streamflow assimilation using the EnKF algorithm with the best parameter settings. In this real data assimilation scenario, the patterns of parameter convergence to the posterior distributions are similar to those generated in the synthetic experiment, but the derived posterior parameter distributions vary greatly from the synthetic experiment due to the assimilation of different streamflow data. The first two parameters relating to the soil moisture storage capacity rapidly converge to the posterior distributions; in comparison, the other three parameters are less identifiable. This is because the parameter evolution in the EnKF follows a random walk by adding a small random perturbation at each time step, such a parameter sampling scheme may result in an over-dispersion of parameter samples.

To address the potential issue of the random walk parameter sampling scheme, we also used an alternative parameter sampling approach that estimated the posterior importance weight for each parameter ensemble member based on the corresponding distance from the observation in the state space, leading to a weighted parameter sample. Such a weighted parameter sampling approach is able to reduce the parameter uncertainty by facilitating the parameter convergence to posterior distributions in comparison with the random walk parameter sampling. Figure 8 shows the evolution of model parameters by using the weighted parameter sampling approach.

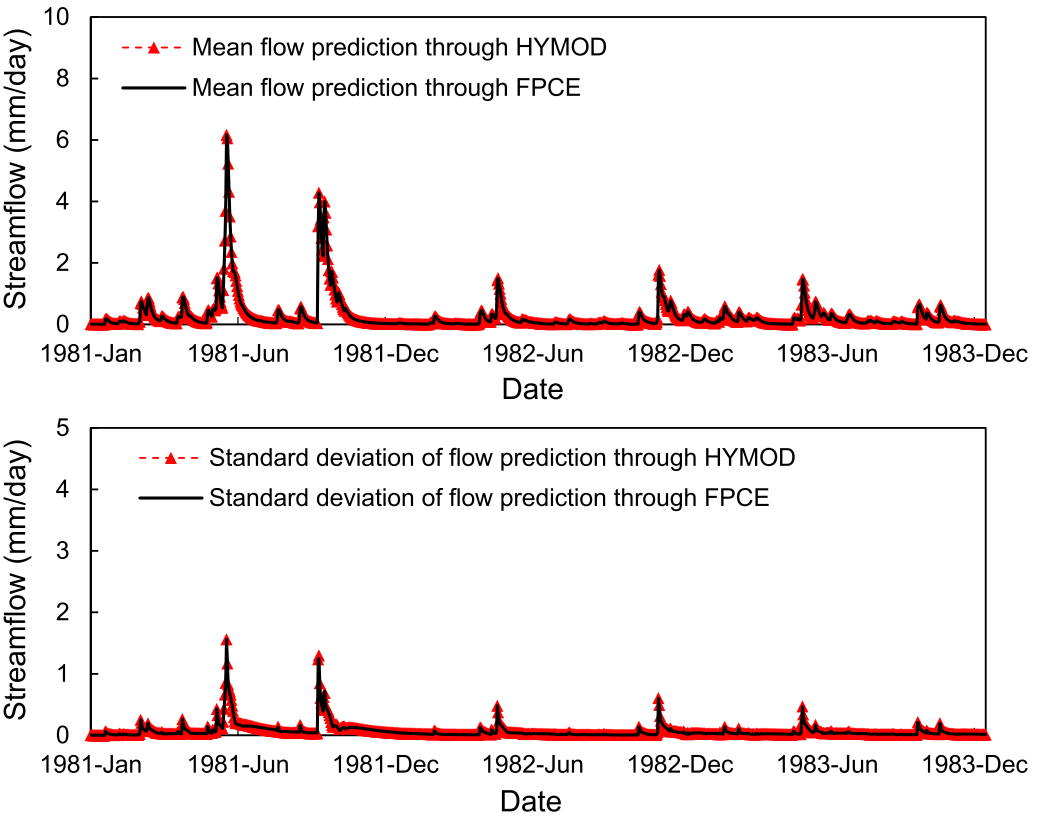

Figure 11. Comparison of probabilistic streamflow time series generated through HYMOD and FPCE.

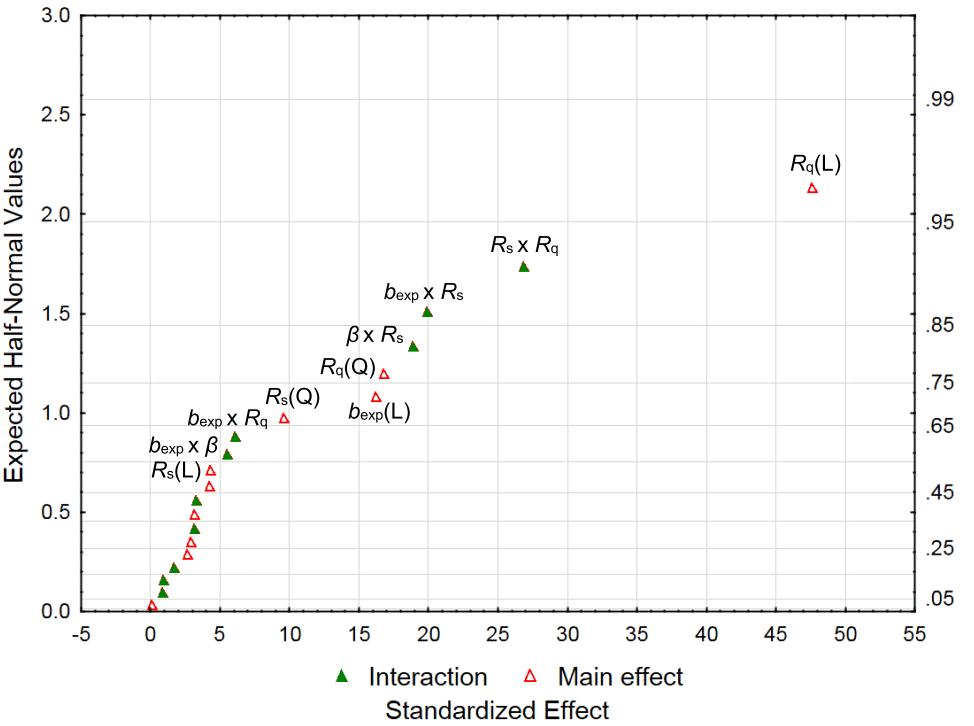

Figure 12. Probability plot of the 10 most significant effects.

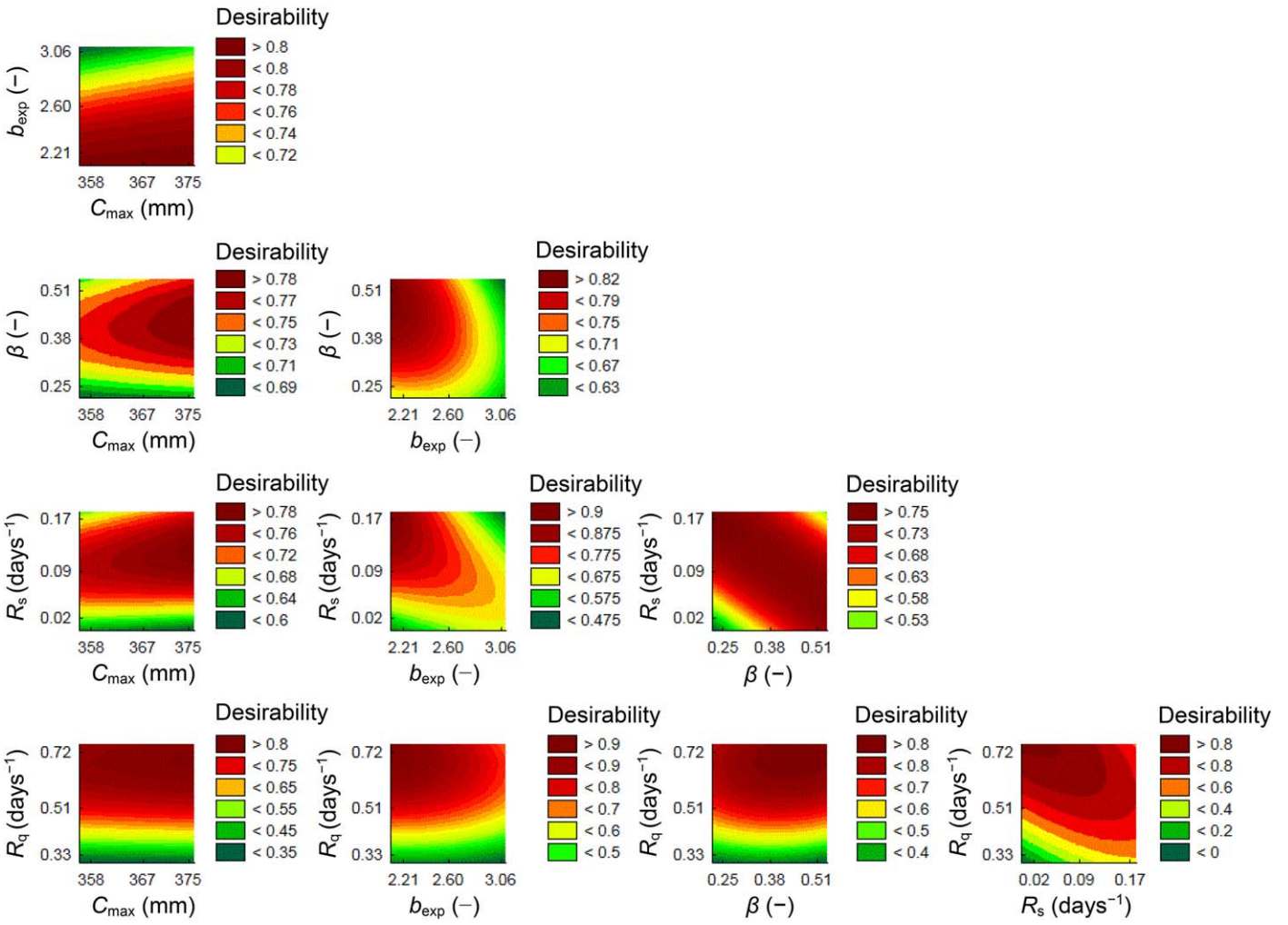

Figure 13. Desirability of predicted response for pairwise parameter interactions.

Results indicate that all parameters rapidly converge to their posterior distributions with a significant reduction of uncertainty. Thus, the weighted parameter sampling approach can be used as a potential extension of the random walk approach to enhance the identifiability and to reduce the uncertainty in the parameter estimation by using the EnKF.

4.3. Quantification of Predictive Uncertainty

The FPCE was used in this study to efficiently produce probabilistic streamflow predictions through a forward propagation of parameter uncertainties. Figure 9 explicitly presents the posterior parameter distributions by assimilating streamflow observations. The Kolmogorov-Smirnov goodness-of-fit statistic was used to perform a hypothesis testing for normality of posterior parameter distributions with a sample size of 100. The derived p-values for model parameters C_{max}, b_{exp}, β, R_s, and R_q are 0.20, 0.20, 0.02, 0.03, and 0.20, respectively. The test rejects the hypothesis of normality for the posterior distributions of parameters β and R_s since their p-values are less than the significance level of 0.05. In fact, when more observations are assimilated with Gaussian errors as time passes, the posterior parameter distributions derived through data assimilation may become closer to Gaussian distributions, but not well approximated by normal Gaussian probability density functions (Zhou et al., 2011).

To examine the robustness in the assessment of the posterior distributions of model parameters, the impacts of sampling fluctuations on the estimation of the non-Gaussian characteristics of the posterior distributions were investigated by performing repeated simulation runs. As shown in Figure 10, the derived

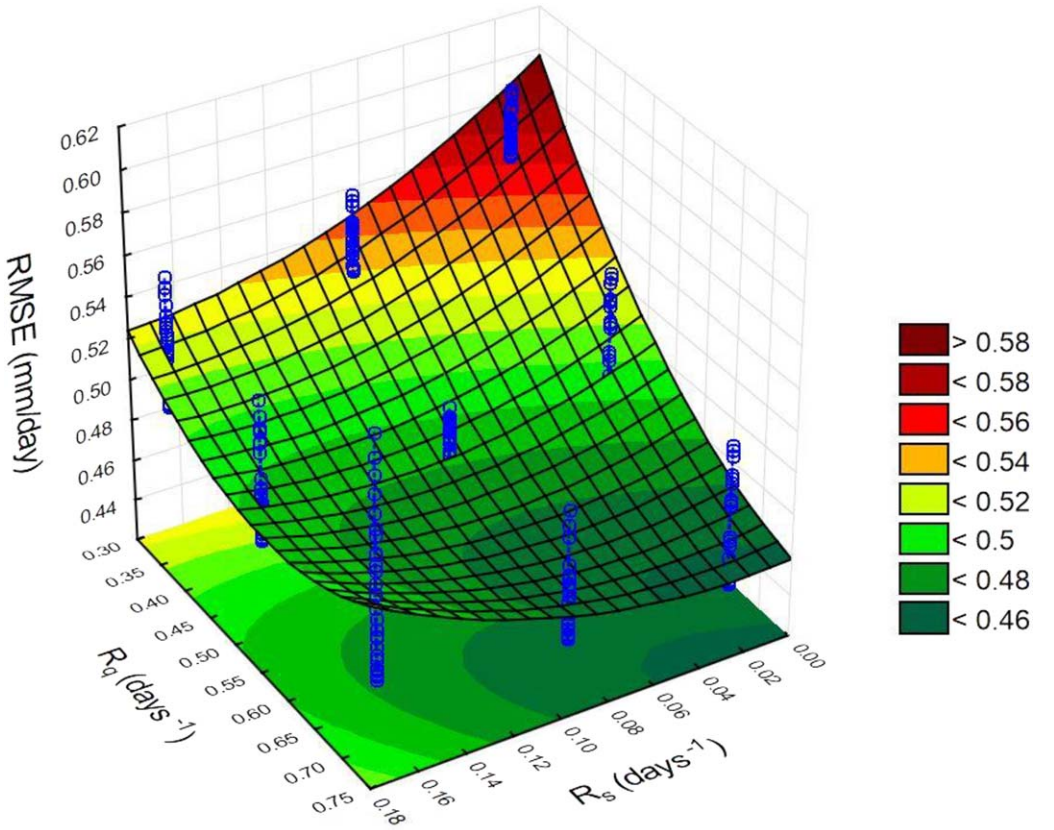

Figure 14. Fitted surfaces of RMSE for the most significant interaction. R_q and R_s represent the quick- and slow-flow tank parameters, respectively. The blue circles represent the samples of RMSE derived under nine parameter combinations.

posterior distributions of model parameters are different from those shown in Figure 9, indicating that the non-Gaussian characteristics of posterior parameter distributions vary due to the sampling fluctuations. Nevertheless, the characteristics of the high-frequency parameter values are similar while performing repeated simulation runs. For instance, the parameter β always has the value of approximately 0.35 with the highest frequency although its non-Gaussian characteristics of the posterior distributions are different under repeated simulation runs. These findings reveal that the sampling fluctuations have a considerable influence on the estimation of the non-Gaussian characteristics of the posterior distributions but have little effect on the identification of the high-frequency parameter values.

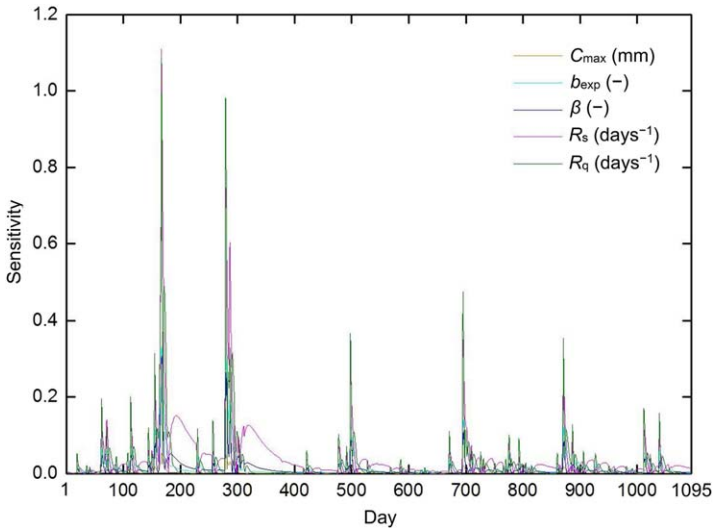

Figure 15. Temporal variation in parameter sensitivity derived by using the FPCE with time-varying coefficients.

Gaussian anamorphosis was used to transform the posterior parameter distributions into normal distributions in order to quantify the uncertainty in streamflow predictions through the FPCE. A five-dimensional second-order FPCE was used in this study to characterize predictive uncertainties because the HYMOD consists of five random parameters. As shown in Figure 11, the probabilistic streamflow time series derived from the FPCE agree well with the HYMOD simulation results. This verifies that the FPCE can be used as an efficient alternative to the HYMOD for producing probabilistic streamflow predictions.

4.4. Sensitivities of Model Parameters and Their Interactions

The FPCE is capable not only of quantifying predictive uncertainties, but also of examining the sensitivities of model parameters and their

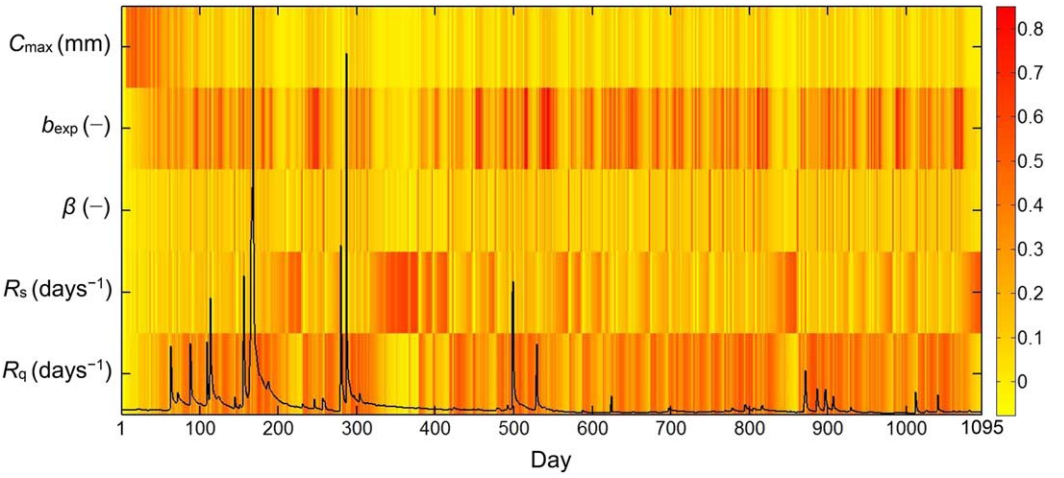

Figure 16. Temporal variation in parameter sensitivity derived by using the variance-based sensitivity analysis.

interactions. As shown in Figure 12, the residence time of the quick-flow tank, denoted as R_q, has the greatest effect on the predictive accuracy. This indicates that the predicted daily streamflow is highly sensitive to the variation of the residence time of the quick-flow tank, and thus the quick-flow tank parameter plays a crucial role in streamflow predictions in the Guadalupe River basin. In addition, the interaction between the quick- and slow-flow tank parameters has the most significant contribution to the predictive performance.

Figure 13 presents all pairwise parameter interactions and the resulting desirability of predicted response by using RMSE. Results reveal that the pairwise interactions between the quick-flow tank parameter R_q and the other model parameters tend to produce highly desirable response values, especially when interacting with the degree of spatial variability of soil moisture capacity and with the residence time of the slow-flow tank. To further examine complex parameter interactions affecting the predictive accuracy, Figure 14 depicts the fitted surface of RMSE derived from the most significant interaction between the quick- and slow-flow tank parameters. Since the second-order FPCE was used to represent the uncertainty in streamflow predictions, a three-level FDA was performed to examine the pairwise interactions between model parameters affecting the predictive accuracy. As a result, a set of the RMSE values were generated through streamflow predictions under all combinations (i.e., $3 \times 3 = 9$) of two parameters with each having three scenarios, leading to a fitted surface of RMSE for the pairwise parameter interactions. As shown in Figure 14, the blue circles represent the samples of RMSE derived under nine parameter combinations accordingly. It is indicated that the pairwise interaction would achieve better predictive accuracy with smaller RMSE values while increasing the values of the quick-flow tank parameter and decreasing the values of the slow-flow tank parameter simultaneously. These findings provide insights into the parameter interactions that affect model performance.

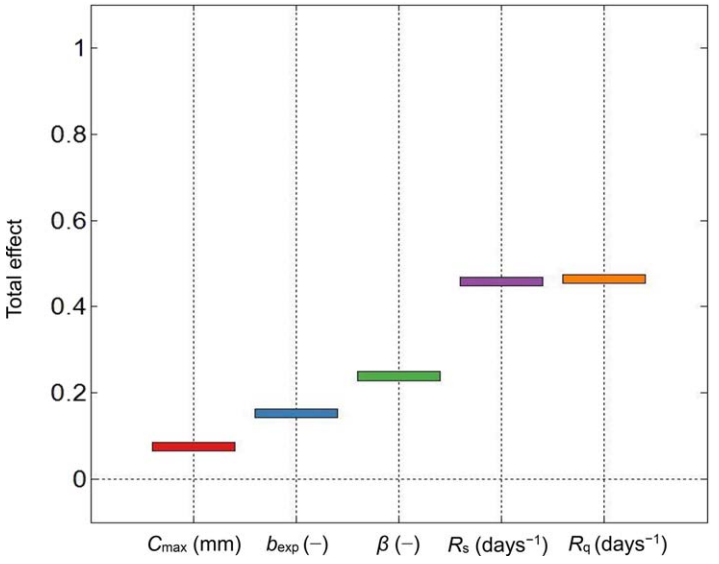

Figure 17. Total effects of model parameters derived by using the variance-based sensitivity analysis.

In this study, parameter sensitivities are calculated as the absolute values of the FPCE coefficients. The larger the FPCE coefficient, the more sensitive the corresponding model parameter. Thus, the FPCE with time-varying coefficients can be used to reveal the temporal variation in the parameter sensitivity. As shown in Figure 15, parameter sensitivities vary over time due to the changing hydrologic conditions. The predictive performance is more sensitive to the variation in the quick-flow tank parameter and the spatial variability of soil moisture

capacity when heavy rainfall occurs on days 167 (44.77 mm), 279 (93.23 mm), 286 (29.58 mm), 498 (41.57 mm), 695 (48.18 mm), 870 (28.06 mm), and 871 (26.27 mm).

To examine the robustness of the results obtained from the FPCE, the Sobol' method was also used to perform the variance-based measures of parameter sensitivities. As shown in Figure 16, the parameters relating to the residence time of the quick-flow tank R_q, the degree of spatial variability of soil moisture capacity b_{exp}, and the residence time of the slow-flow tank R_s have considerable impacts on the performance of streamflow predictions, and their sensitivities vary continuously at a daily time step. These results are in good agreement with those reported in Figure 12, indicating that the results derived from the FPCE are robust and reliable in comparison with the variance-based global sensitivity analysis. In terms of the detection of parameter interactions, the variance-based sensitivity analysis method can only be used to provide a total interaction effect of model parameters, as shown in Figure 17. In comparison, the FPCE has the advantage of revealing the pairwise parameter interactions affecting the performance of streamflow predictions, which provides meaningful insights into the exploration of the parameter space and reveals spatial variations in the predictive accuracy.

5. Conclusions

In this study, we developed a unified data assimilation framework for improving the robustness in ensemble streamflow predictions. Statistical pre-processing of assimilation experiments was conducted through the FDA to identify the best EnKF settings with maximized predictive performance. When the posterior distributions of hydrologic model parameters were estimated through the EnKF data assimilation experiment, statistical post-processing analysis was then performed through the FPCE to efficiently quantify parameter interactions and predictive uncertainties. In addition, the Gaussian anamorphosis was performed to build a seamless bridge between data assimilation and uncertainty quantification through transforming posterior parameter distributions into normal distributions. Such a unified computational framework improves the robustness of sequential data assimilation by using statistical pre- and post-processing techniques, and strengthens our capability in providing probabilistic streamflow predictions.

Both synthetic and real data assimilation experiments were conducted to demonstrate feasibility and applicability of the proposed computational framework in the Guadalupe River basin, Texas. Results obtained from the synthetic experiment verify the ability of the EnKF to properly estimate the posterior distributions of model parameters. In comparison, the maximum soil moisture storage capacity parameter C_{max} and the degree of spatial variability of soil moisture capacity b_{exp} are more identifiable, and they rapidly converge to the posterior target distributions in the streamflow assimilation process. The EnKF can thus be applied to the real data assimilation experiment for estimating model parameters and state variables. According to the results obtained from the statistical pre-processing of assimilation experiments with real streamflow observations, the precipitation error parameter has the most significant impact on the predictive accuracy, and its interaction with the streamflow observation error parameter varies dynamically depending on the settings of the potential evapotranspiration error parameter. Such an interaction analysis reveals meaningful information for advancing our understanding of the EnKF data assimilation system and for maximizing the predictive performance.

Since the posterior parameter distributions derived through data assimilation can hardly be characterized by certain probability distributions, the Gaussian anamorphosis was used to transform posterior parameter distributions into normal distributions for revealing predictive uncertainties and parameter sensitivities. Our findings reveal that the quick-flow tank parameter R_q has the largest effect on the predictive performance, and its interactions with the other parameters tend to achieve better predictive accuracy. In addition, parameter sensitivities vary over time due to the changing hydrologic characteristics. The predictive performance is more sensitive to parameter variations for the days when heavy rainfall occurs.

The proposed statistical pre- and post-processing of data assimilation experiments are necessary to enhance the robustness of hydrologic ensemble predictions. Thus, the unified data assimilation framework has significant potential for performing robust hydroclimatic forecasting. The effectiveness and efficiency of

the proposed methodology will be examined by using highly parameterized and complex hydroclimatic models in future studies.

Acknowledgments
This research was supported by The Hong Kong Polytechnic University Start-up Grant (1-ZE8S). The daily hydrological data for the Guadalupe River basin were collected from the U.S. MOPEX data set, and were provided as Supporting Information. The authors appreciate Dr. Francesca Pianosi for providing the Matlab toolbox to perform the global sensitivity analysis. The authors would also like to express their sincere gratitude to the editor and three anonymous reviewers for their constructive comments and suggestions.

References

Ajami, N. K., Duan, Q., & Sorooshian, S. (2007). An integrated hydrologic Bayesian multimodel combination framework: Confronting input, parameter, and model structural uncertainty in hydrologic prediction. *Water Resources Research*, *43*, W01403. https://doi.org/10.1029/2005WR004745

Bulygina, N., & Gupta, H. (2011). Correcting the mathematical structure of a hydrological model via Bayesian data assimilation. *Water Resources Research*, *47*, W05514. https://doi.org/10.1029/2010WR009614

Cammalleri, C., & Ciraolo, G. (2012). State and parameter update in a coupled energy/hydrologic balance model using ensemble Kalman filtering. *Journal of Hydrology*, *416–417*, 171–181. https://doi.org/10.1016/j.jhydrol.2011.11.049

Ciriello, V., Federico, V. D., Riva, M., Cadini, F., Sanctis, J. D., Zio, E., & Guadagnini, A. (2013). Polynomial chaos expansion for global sensitivity analysis applied to a model of radionuclide migration in a randomly heterogeneous aquifer. *Stochastic Environmental Research and Risk Assessment*, *27*(4), 945–954. https://doi.org/10.1007/s00477-012-0616-7

Clark, M. P., Rupp, D. E., Woods, R. A., Zheng, X., Ibbitt, R. P., Slater, A. G., et al. (2008). Hydrological data assimilation with the ensemble Kalman filter: Use of streamflow observations to update states in a distributed hydrological model. *Advances in Water Resources*, *31*(10), 1309–1324. https://doi.org/10.1016/j.advwatres.2008.06.005

Crow, W. T., & Loon, E. V. (2006). Impact of incorrect model error assumptions on the sequential assimilation of remotely sensed surface soil moisture. *Journal of Hydrometeorology*, *7*(3), 421–432. https://doi.org/10.1175/JHM499.1

Dai, C., Xue, L., Zhang, D., & Guadagnini, A. (2016). Data-worth analysis through probabilistic collocation-based Ensemble Kalman Filter. *Journal of Hydrology*, *540*, 488–503. https://doi.org/10.1016/j.jhydrol.2016.06.037

Dai, H., & Ye, M. (2015). Variance-based global sensitivity analysis for multiple scenarios and models with implementation using sparse grid collocation. *Journal of Hydrology*, *528*, 286–300. https://doi.org/10.1016/j.jhydrol.2015.06.034

DeChant, C. M., & Moradkhani, H. (2012). Examining the effectiveness and robustness of sequential data assimilation methods for quantification of uncertainty in hydrologic forecasting. *Water Resources Research*, *48*, W04518. https://doi.org/10.1029/2011WR011011

De Lannoy, G. J. M., Houser, P. R., Verhoest, N. E. C., & Pauwels, V. R. N. (2009). Adaptive soil moisture profile filtering for horizontal information propagation in the independent column-based CLM2.0. *Journal of Hydrometeorology*, *10*, 766–779. https://doi.org/10.1175/2008JHM1037.1

De Lannoy, G. J. M., & Reichle, R. H. (2016). Assimilation of SMOS brightness temperatures or soil moisture retrievals into a land surface model. *Hydrology and Earth System Sciences*, *120*, 4895–4911. https://doi.org/10.5194/hess-20-4895-2016

Duan, Q., Schaake, J., Andréassian, V., Franks, S., Goteti, G., Gupta, H. V., et al. (2006). Model parameter estimation experiment (MOPEX): An overview of science strategy and major results from the second and third workshops. *Journal of Hydrology*, *320*(1–2), 3–17. https://doi.org/10.1016/j.jhydrol.2005.07.031

Evensen, G. (1994). Sequential data assimilation with a nonlinear quasi-geostrophic model using Monte Carlo methods to forecast error statistics. *Journal of Geophysical Research*, *99*(C5), 10143–10162. https://doi.org/10.1029/94JC00572

Evensen, G. (2003). The Ensemble Kalman Filter: Theoretical formulation and practical implementation. *Ocean Dynamics*, *53*(4), 343–367. https://doi.org/10.1007/s10236-003-0036-9

Fajraoui, N., Ramasomanana, F., Younes, A., Mara, T. A., Ackerer, P., & Guadagnini, A. (2011). Use of global sensitivity analysis and polynomial chaos expansion for interpretation of nonreactive transport experiments in laboratory-scale porous media. *Water Resources Research*, *47*, W02521. https://doi.org/10.1029/2010WR009639

Gharamti, M. E., Ait-El-Fquih, B., & Hoteit, I. (2015). An iterative ensemble Kalman filter with one-step-ahead smoothing for state-parameters estimation of contaminant transport models. *Journal of Hydrology*, *527*, 442–457. https://doi.org/10.1016/j.jhydrol.2015.05.004

Gharamti, M. E., Hoteit, I., & Valstar, J. (2013). Dual states estimation of a subsurface flow-transport coupled model using ensemble Kalman filtering. *Advances in Water Resources*, *60*, 75–88. https://doi.org/10.1016/j.advwatres.2013.07.011

Johnson, R. A., & Wichern, D. W. (1988). *Applied multivariate statistical analysis*. Englewood Cliffs, NJ: Prentice-Hall.

Khan, U. T., & Valeo, C. (2016). Short-term peak flow rate prediction and flood risk assessment using fuzzy linear regression. *Journal of Environmental Informatics*, *28*(2), 71–89. https://doi.org/10.3808/jei.201600345

Li, H., & Zhang, D. (2007). Probabilistic collocation method for flow in porous media: Comparisons with other stochastic methods. *Water Resources Research*, *43*, W09409. https://doi.org/10.1029/2006WR005673

Liu, D., Mishra, A. K., & Yu, Z. (2016). Evaluating uncertainties in multi-layer soil moisture estimation with support vector machines and ensemble Kalman filtering. *Journal of Hydrology*, *538*, 243–255. https://doi.org/10.1016/j.jhydrol.2016.04.021

McMillan, H. K., Hreinsson, E. Ö., Clark, M. P., Singh, S. K., Zammit, C., & Uddstrom, M. J. (2013). Operational hydrological data assimilation with the recursive ensemble Kalman filter. *Hydrology and Earth System Sciences*, *17*(1), 21–38. https://doi.org/10.5194/hess-17-21-2013

Montgomery, D. (2000). *Design and analysis of experiments* (5th ed.). New York, NY: John Wiley & Sons.

Montgomery, D. C., & Runger, G. C. (2013). *Applied statistics and probability for engineers* (6th ed.). Hoboken, NJ: John Wiley & Sons.

Moore, R. J. (2007). The PDM rainfall-runoff model. *Hydrology and Earth System Sciences*, *11*(1), 483–499. https://doi.org/10.5194/hess-11-483-2007.

Moradkhani, H., Sorooshian, S., Gupta, H. V., & Houser, P. R. (2005). Dual state–parameter estimation of hydrological models using ensemble Kalman filter. *Advances in Water Resources*, *28*(2), 135–147. https://doi.org/10.1016/j.advwatres.2004.09.002

Müller, F., Jenny, P., & Meyer, D. W. (2011). Probabilistic collocation and lagrangian sampling for advective tracer transport in randomly heterogeneous porous media. *Advances in Water Resources*, *34*(12), 1527–1538. https://doi.org/10.1016/j.advwatres.2011.09.005

Ockerman, D. J., & Slattery, R. N. (2008). Streamflow conditions in the Guadalupe River Basin, south-central Texas, water years 1987–2006—An assessment of streamflow gains and losses and relative contribution of major springs to streamflow. *U.S. Geological Survey Scientific Investigations Report*, *2008–5165*, 22 p.

Panzeri, M., Riva, M., Guadagnini, A., & Neuman, S. P. (2014). Comparison of Ensemble Kalman Filter groundwater-data assimilation methods based on stochastic moment equations and Monte Carlo simulation. *Advances in Water Resources*, *66*, 8–18. https://doi.org/10.1016/j.advwatres.2014.01.007

Pathiraja, S., Marshall, L., Sharma, A., & Moradkhani, H. (2016a). Hydrologic modeling in dynamic catchments: A data assimilation approach. *Water Resources Research*, *52*, 3350–3372. https://doi.org/10.1002/2015WR017192

Pathiraja, S., Marshall, L., Sharma, A., & Moradkhani, H. (2016b). Detecting non-stationary hydrologic model parameters in a paired catchment system using data assimilation. *Advances in Water Resources*, *94*, 103–119. https://doi.org/10.1016/j.advwatres.2016.04.021

Pauwels, V. R. N., & De Lannoy, G. J. M. (2009). Ensemble-based assimilation of discharge into rainfall-runoff models: A comparison of approaches to mapping observational information to state space. *Water Resources Research*, *45*, W08428. https://doi.org/10.1029/2008WR007590

Pauwels, V. R. N., De Lannoy, G. J. M., Hendricks Franssen, H. J., & Vereecken, H. (2013). Simultaneous estimation of model state variables and observation and forecast biases using a two-stage hybrid Kalman filter. *Hydrology and Earth System Science*, *17*, 3499–3521. https://doi.org/10.5194/hess-17-3499-2013

Pianosi, F., & Wagener, T. (2016). Understanding the time-varying importance of different uncertainty sources in hydrological modelling using global sensitivity analysis. *Hydrological Processes*, *30*(22), 3991–4003. https://doi.org/10.1002/hyp.10968

Rafieeinasab, A., Seo, D.-J., Lee, H., & Kim, S. (2014). Comparative evaluation of maximum likelihood ensemble filter and ensemble Kalman filter for real-time assimilation of streamflow data into operational hydrologic models. *Journal of Hydrology*, *519*(Part D), 2663–2675. https://doi.org/10.1016/j.jhydrol.2014.06.052

Rajabi, M. M., Ataie-Ashtiani, B., & Simmons, C. T. (2015). Polynomial chaos expansions for uncertainty propagation and moment independent sensitivity analysis of seawater intrusion simulations. *Journal of Hydrology*, *520*, 101–122. https://doi.org/10.1016/j.jhydrol.2014.11.020

Raleigh, M. S., Lundquist, J. D., & Clark, M. P. (2015). Exploring the impact of forcing error characteristics on physically based snow simulations within a global sensitivity analysis framework. *Hydrology and Earth System Sciences*, *19*, 3153–3179. https://doi.org/10.5194/hess-19 3153-2015

Randrianasolo, A., Thirel, G., Ramos, M. H., & Martin, E. (2014). Impact of streamflow data assimilation and length of the verification period on the quality of short-term ensemble hydrologic forecasts. *Journal of Hydrology*, *519*(Part D), 2676–2691. https://doi.org/10.1016/j.jhydrol.2014.09.032

Rasmussen, J., Madsen, H., Jensen, K. H., & Refsgaard, J. C. (2015). Data assimilation in integrated hydrological modeling using ensemble Kalman filtering: Evaluating the effect of ensemble size and localization on filter performance. *Hydrology and Earth System Sciences*, *19*(7), 2999–3013. https://doi.org/10.5194/hess-19-2999-2015

Rasmussen, J., Madsen, H., Jensen, K. H., & Refsgaard, J. C. (2016). Data assimilation in integrated hydrological modelling in the presence of observation bias. *Hydrology and Earth System Sciences*, *20*, 2103–2118. https://doi.org/10.5194/hess-20-2103-2016

Renard, B., Kavetski, D., Kuczera, G., Thyer, M., & Franks, S. W. (2010). Understanding predictive uncertainty in hydrologic modeling: The challenge of identifying input and structural errors. *Water Resources Research*, *46*, W05521. https://doi.org/10.1029/2009WR008328

Ryu, D., Crow, W. T., Zhan, X., & Jackson, T. J. (2009). Correcting unintended perturbation biases in hydrologic data assimilation. *Journal of Hydrometeorology*, *10*, 734–750. https://doi.org/10.1175/2008JHM1038.1

Sadegh, M., & Vrugt, J. A. (2013). Bridging the gap between GLUE and formal statistical approaches: Approximate Bayesian computation. *Hydrology and Earth System Sciences*, *17*, 4831–4850. https://doi.org/10.5194/hess-17-4831-2013

Samuel, J., Coulibaly, P., Dumedah, G., & Moradkhani, H. (2014). Assessing model state and forecasts variation in hydrologic data assimilation. *Journal of Hydrology*, *513*, 127–141. https://doi.org/10.1016/j.jhydrol.2014.03.048

Schöniger, A., Nowak, W., & Hendricks Franssen, H. J. (2012). Parameter estimation by ensemble Kalman filters with transformed data: Approach and application to hydraulic tomography. *Water Resources Research*, *48*, W04502. https://doi.org/10.1029/2011WR010462

Sharif, H. O., Hassan, A. A., Bin-Shafique, S., Xie, H., & Zeitler, J. (2010). Hydrologic modeling of an extreme flood in the Guadalupe River in Texas. *Journal of American Water Resources. Association*, *46*(5), 881–891. https://doi.org/10.1111/j.1752-1688.2010.00459.x

Sochala, P., & Le Maître, O. P. (2013). Polynomial Chaos expansion for subsurface flows with uncertain soil parameters. *Advances in Water Resources*, *62*, 139–154. https://doi.org/10.1016/j.advwatres.2013.10.003

Song, X., Zhang, J., Zhan, C., Xuan, Y., Ye, M., & Xu, C. (2015). Global sensitivity analysis in hydrological modeling: Review of concepts, methods, theoretical framework, and applications. *Journal of Hydrology*, *523*, 739–757. https://doi.org/10.1016/j.jhydrol.2015.02.013

Sun, A. Y., Morris, A., & Mohanty, S. (2009). Comparison of deterministic ensemble Kalman filters for assimilating hydrogeological data. *Advances in Water Resources*, *32*(2), 280–292. https://doi.org/10.1016/j.advwatres.2008.11.006

Tatang, M. A., Pan, W., Prinn, R. G., & McRae, G. J. (1997). An efficient method for parametric uncertainty analysis of numerical geophysical models. *Journal of Geophysical Research*, *102*(D18), 21925–21932. https://doi.org/10.1029/97JD01654

Thiboult, A., & Anctil, F. (2015). On the difficulty to optimally implement the Ensemble Kalman filter: An experiment based on many hydrological models and catchments. *Journal of Hydrology*, *529*(Part 3), 1147–1160. https://doi.org/10.1016/j.jhydrol.2015.09.036

Wang, D., Chen, Y., & Cai, X. (2009). State and parameter estimation of hydrologic models using the constrained ensemble Kalman filter. *Water Resources Research*, *45*, W11416, https://doi.org/10.1029/2008WR007401

Wang, S., Huang, G. H., Baetz, B. W., & Ancell, B. C. (2017). Towards robust quantification and reduction of uncertainty in hydrologic predictions: Integration of particle Markov chain Monte Carlo and factorial polynomial chaos expansion. *Journal of Hydrology*, *548*, 484–497. https://doi.org/10.1016/j.jhydrol.2017.03.027

Wang, S., Huang, G. H., Baetz, B. W., & Huang, W. (2015a). A polynomial chaos ensemble hydrologic prediction system for efficient parameter inference and robust uncertainty assessment. *Journal of Hydrology*, *530*, 716–733. https://doi.org/10.1016/j.jhydrol.2015.10.021

Wang, S., Huang, G. H., Huang, W., Fan, Y. R., & Li, Z. (2015b). A fractional factorial probabilistic collocation method for uncertainty propagation of hydrologic model parameters in a reduced dimensional space. *Journal of Hydrology*, *529*(Part 3), 1129–1146. https://doi.org/10.1016/j.jhydrol.2015.09.034

Wiener, N. (1938). The Homogeneous Chaos. *American Journal of Mathematics*, *60*(4), 897–936. https://doi.org/10.2307/2371268

Xie, X., & Zhang, D. (2010). Data assimilation for distributed hydrological catchment modeling via ensemble Kalman filter. *Advances in Water Resources*, *33*(6), 678–690. https://doi.org/10.1016/j.advwatres.2010.03.012

Xiu, D., & Karniadakis, G. (2002). The Wiener–Askey polynomial chaos for stochastic differential equations. *SIAM Journal of Scientific Computing*, *24*(2), 619–644. https://doi.org/10.1137/S1064827501387826

Xu, T., Valocchi, A. J., Ye, M., & Liang, F. (2017). Quantifying model structural error: Efficient Bayesian calibration of a regional groundwater flow model using surrogates and a data-driven error model. *Water Resources Research*, *53*, 4084–4105. https://doi.org/10.1002/2016WR019831

Yin, J., Zhan, X., Zheng, Y., Hain, C. R., Liu, J., & Fang, L. (2015). Optimal ensemble size of ensemble Kalman filter in sequential soil moisture data assimilation. *Geophysical Research Letters*, *42*, 6710–6715. https://doi.org/10.1002/2015GL063366

Young, P. C. (2013). Hypothetico-inductive data-based mechanistic modeling of hydrological systems. *Water Resources Research*, *49*, 915–935. https://doi.org/10.1002/wrcr.20068

Zhang, D., Madsen, H., Ridler, M. E., Kidmose, J., Jensen, K. H., & Refsgaard, J. C. (2016). Multivariate hydrological data assimilation of soil moisture and groundwater head. *Hydrology and Earth System Sciences*, *20*, 4341–4357. https://doi.org/10.5194/hess-20-4341-2016

Zhang, H., Hendricks Franssen, H. J., Han, X., Vrugt, J. A., & Vereecken, H. (2017). State and parameter estimation of two land surface models using the ensemble Kalman filter and the particle filter. *Hydrology and Earth System Sciences*, *21*, 4927–4958. https://doi.org/10.5194/hess-21-4927-2017

Zhou, H., Gómez-Hernández, J. J., Hendricks Franssen, H. J., & Li, L. (2011). An approach to handling non-Gaussianity of parameters and state variables in ensemble Kalman filtering. *Advances in Water Resources*, *34*, 844–864. https://doi.org/10.1016/j.advwatres.2011.04.014